(12) INTERNATIONAL APPLICATION PUBLISHED UNDER THE PATENT COOPERATION TREATY (PCT)

(19) World Intellectual Property Organization
International Bureau

(43) International Publication Date
13 November 2025 (13.11.2025)

WIPO | PCT

(10) International Publication Number
WO 2025/235450 A1

(51) International Patent Classification:
C02F 1/58 (2023.01) *C25B 3/25* (2021.01)
C25B 1/29 (2021.01) *A62D 3/115* (2007.01)
C25B 1/30 (2006.01) *A62D 3/34* (2007.01)
C25B 3/23 (2021.01) *C02F 1/467* (2023.01)

(21) International Application Number:
PCT/US2025/027892

(22) International Filing Date:
06 May 2025 (06.05.2025)

(25) Filing Language: English

(26) Publication Language: English

(30) Priority Data:
63/643,280 06 May 2024 (06.05.2024) US

(71) Applicant: **WISCONSIN ALUMNI RESEARCH FOUNDATION** [US/US]; 614 Walnut Street, Madison, Wisconsin 53726 (US).

(72) Inventors: **JIN, Song**; 1101 University Ave., Madison, Wisconsin 53706 (US). **MICHAEL, Katelyn**; 1101 University Ave., Madison, Wisconsin 53706 (US).

(74) Agent: **GULMEN, Tolga S.**; QUARLES & BRADY LLP, 33 East Main Street, Suite 900, Madison, Wisconsin 53703 (US).

(81) Designated States *(unless otherwise indicated, for every kind of national protection available)*: AE, AG, AL, AM, AO, AT, AU, AZ, BA, BB, BG, BH, BN, BR, BW, BY, BZ, CA, CH, CL, CN, CO, CR, CU, CV, CZ, DE, DJ, DK, DM, DO, DZ, EC, EE, EG, ES, FI, GB, GD, GE, GH, GM, GT, HN, HR, HU, ID, IL, IN, IQ, IR, IS, IT, JM, JO, JP, KE, KG, KH, KN, KP, KR, KW, KZ, LA, LC, LK, LR, LS, LU, LY,

(54) Title: TANDEM OXIDATIVE PROCESSES TO DEGRADE PER- AND POLYFLUOROALKYL SUBSTANCES

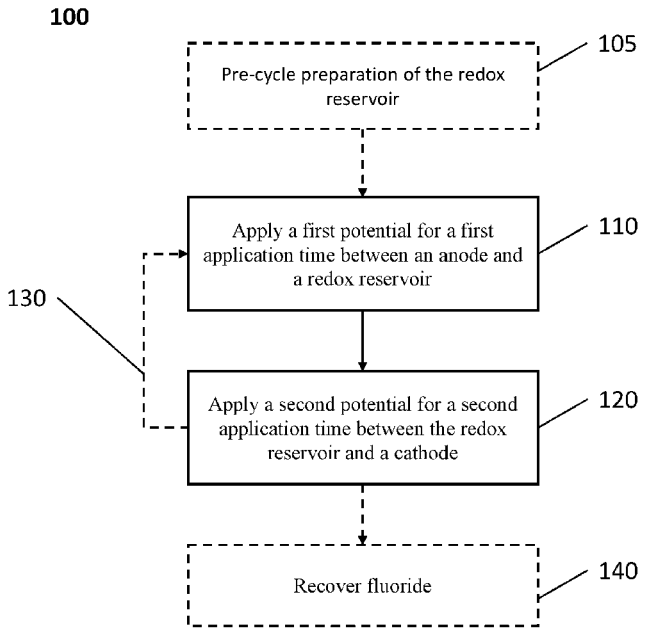

FIG. 10

(57) Abstract: Disclosed herein are tandem oxidative process for the degradation of per- and polyfluoroalkyl substances (PFAS). PFAS may be degraded with an electrochemical cell comprising an anode comprising a persulfate catalyst, a cathode comprising a hydrogen peroxide catalyst, a redox reservoir, a Fenton activator, and an acidic to neutral electrolyte having sulfate and at least one perfluorinated or polyfluorinated alkyl substance (PFAS) therein. The anode and redox reservoir are in electrical communication and the redox reservoir and the cathode are in electrical communication. Further, the electrochemical cell is configured to have a first potential applied between the anode and the redox reservoir for a first application time and a second potential applied to the redox reservoir and the cathode for a second application time that is different from the first application time. Methods for degrading PFAS are also disclosed.

WO 2025/235450 A1

[Continued on next page]

MA, MD, MG, MK, MN, MU, MW, MX, MY, MZ, NA, NG, NI, NO, NZ, OM, PA, PE, PG, PH, PL, PT, QA, RO, RS, RU, RW, SA, SC, SD, SE, SG, SK, SL, ST, SV, SY, TH, TJ, TM, TN, TR, TT, TZ, UA, UG, US, UY, UZ, VC, VN, WS, ZA, ZM, ZW.

(84) **Designated States** *(unless otherwise indicated, for every kind of regional protection available)*: ARIPO (BW, CV, GH, GM, KE, LR, LS, MW, MZ, NA, RW, SC, SD, SL, ST, SZ, TZ, UG, ZM, ZW), Eurasian (AM, AZ, BY, KG, KZ, RU, TJ, TM), European (AL, AT, BE, BG, CH, CY, CZ, DE, DK, EE, ES, FI, FR, GB, GR, HR, HU, IE, IS, IT, LT, LU, LV, MC, ME, MK, MT, NL, NO, PL, PT, RO, RS, SE, SI, SK, SM, TR), OAPI (BF, BJ, CF, CG, CI, CM, GA, GN, GQ, GW, KM, ML, MR, NE, SN, TD, TG).

Published:

— *with international search report (Art. 21(3))*

TANDEM OXIDATIVE PROCESSES TO DEGRADE PER- AND POLYFLUOROALKYL SUBSTANCES

CROSS-REFERENCE TO RELATED APPLICATIONS

This application is related to, claims priority to, and incorporates herein by reference for all purposes U.S. Provisional Patent Application No. 63/643,280, filed May 6, 2024.

STATEMENT REGARDING FEDERALLY SPONSORED RESEARCH

This invention was made with government support under 2219089 awarded by the National Science Foundation. The government has certain rights in the invention.

FIELD OF THE INVENTION

The disclosed technology is generally directed to electrochemical processing of PFAS. More particularly the technology is directed to electrochemical degradation of PFAS.

BACKGROUND OF THE INVENTION

Per- and polyfluoroalkyl substances (PFAS) are a family of persistent and ubiquitous pollutants in drinking water and are widely recognized for their resistance to environmental degradation. The name "PFAS" encompass many compounds with different functional groups and various carbon chain lengths, but they invariably contain C-F bonds, which imparts high stability and thus allows them to accumulate over time in the environment and in the bodies of animals and people, posing health risks. Epidemiological studies have revealed associations between exposure to specific PFAS and a variety of health effects, including altered immune and thyroid function, liver disease, lipid and insulin dysregulation, kidney disease, adverse reproductive and developmental outcomes, and cancer. Mature and implementable technologies exist for adsorption of PFAS from water sources, however if the collected PFAS are not degraded by breaking C-F bonds, the collected PFAS may be reintroduced to the environment. Therefore, degradation technologies that break these C-F bonds are imperative to addressing this global environmental and health concern over PFAS.

Electrochemical approaches are believed to be one of the most practical ways to degrade PFAS but typically suffer from incomplete degradation and low Faradaic efficiencies, meaning the

charge passed is not used for the process of interest. Oxidative destruction can occur directly at the electrode or via advanced oxidation processes (AOPs). One common advanced oxidation process (AOP) is the activation of hydrogen peroxide via metal cations to more potent hydroxyl radicals, known as the Fenton process. Another advanced oxidation process relies on sulfate radicals.

There are previous reports for perfluorooctanoic acid (PFOA) degradation via the Fenton process with oxygen evolution and direct oxidation occurring at the counter electrode. The sulfonate head group of perfluorooctane sulfonate (PFOS) is more electron withdrawing, resulting in the electron abstraction step from the head group being more difficult and rendering hydroxyl radicals ineffective. Therefore, PFOS is generally considered especially more difficult to degrade electrochemically among the various PFAS. Hydroxyl radicals are generally less selective, and can perform hydrogen atom transfer and electron abstraction, while sulfate radicals are more selective and prefer electron abstraction. Electron abstraction processes on their own are also insufficient for complete degradation of PFAS, with the overproduction of persulfate radicals potentially resulting in the sulfonate group being re-introduced to the activated perfluoroalkyl chain. Overall, current electrochemical approaches for degradation of PFAS exhibit poor Faradaic efficiency and complete degradation of PFAS is challenging.

SUMMARY

Disclosed herein are tandem oxidative process for the degradation of per- and polyfluoroalkyl substances (PFAS). PFAS may be degraded with an electrochemical cell comprising an anode comprising a persulfate catalyst, a cathode comprising a hydrogen peroxide catalyst, a redox reservoir, a Fenton activator, and an acidic to neutral electrolyte having sulfate and at least one perfluorinated or polyfluorinated alkyl substance (PFAS) therein. The anode and redox reservoir are in electrical communication and the redox reservoir and the cathode are in electrical communication. Further, the electrochemical cell is configured to have a first potential applied between the anode and the redox reservoir for a first application time and a second potential applied to the redox reservoir and the cathode for a second application time that is different from the first application time.

Another aspect of technology provides for methods for degradation of PFAS. The method comprises applying a first potential for a first application time between an anode comprising a

persulfate catalyst and a redox reservoir in an electrochemical cell having an acidic electrolyte, sulfate, a Fenton activator, and a PFAS therein; and applying a second potential for a second application time after the first application time between the redox reservoir and a cathode comprising a hydrogen peroxide catalyst in the electrochemical cell. The method may further comprise repeating application of the first potential for the first application time and the second potential for the second application time for one or more cycles. The methods may be practiced with the use of the electrochemical cells described herein.

BRIEF DESCRIPTION OF THE DRAWINGS

Non-limiting embodiments of the present invention will be described by way of example with reference to the accompanying figures, which are schematic and are not intended to be drawn to scale. In the figures, each identical or nearly identical component illustrated is typically represented by a single numeral. For purposes of clarity, not every component is labeled in every figure, nor is every component of each embodiment of the invention shown where illustration is not necessary to allow those of ordinary skill in the art to understand the invention.

Figure 1. (A) A reaction scheme shows the chemical reactions of the first step and the second step of the oxidative destruction cycle of PFOS. (B) A schematic drawing of the electrochemical cell shows the connectivity of the anode, cathode, and redox reservoir, as well as the reactions taking place in solution, with the Fenton activator and at the electrodes. (C) A schematic illustrating the interference between persulfate production and an electro-Fenton process if they were directly paired.

Figure 2. H-cell studies were performed to optimize persulfate production at the anode. (A) Plot of Faradaic efficiency(%) vs the concentration of Na_2SO_4. Persulfate is electrochemically produced from sulfate anions in the Na_2SO_4 supporting electrolyte. With increasing concentrations of sulfate, the Faradaic efficiency (%) for persulfate increases as expected for both pH=3 and neutral pH. (B) Plot of Faradaic efficiency (%) vs the applied potential (vs SCE). For 0.4 M Na_2SO_4 at pH=3, the applied potential of 2.78 V vs SCE resulted in 32.7 % FE. (C) Chronoamperometry electrolysis studies show up to 300 ppm of persulfate can be produced with high Faradaic efficiency. (D) In the presence of PFOS, higher potentials are needed for persulfate production, with an optimal potential of approximately 3.3 V, which corresponds to a current of 8-12 mA. (E) A plot of FE% vs charge (C) shows higher potentials are needed to

achieve the same currents with no PFOS present. Constant current operation is beneficial as more charge is passed compared to constant potential (CP) operation. (F) A plot of the concentration of Rhodamine B, a model organic compound, vs time for the activation of persulfate with different activators: FeOCl, $FeSO_4$, or zero valent iron (ZVFe). The concentration of Rhodamine B is quantified using UV-Vis spectrometry. Faster degradation of the Rhodamine B dye is expected with higher radical production. During these studies, 12 mL of 40 ppm Rhodamine B were degraded with 2.5 mM Fenton activator. FeOCl was selected as the preferred Fenton activator. (G) Concentrations of up to 150 ppm of hydrogen peroxide with 45-46% Faradaic efficiency are achievable using a $NiSe_2$ cathode. The reduction is Faradaic efficiency as more charge is passed is due to the known reduction of hydrogen peroxide on the cathode when concentrations increase in solution. Plots of the concentration of Rhodamine B vs time for activator FeOCl (H) and $FeSO_4$ (I) show these are both suitable Fenton activators for hydrogen peroxide, as seen by the complete degradation of 3.5 mL of 40 ppm Rhodamine B in 30 minutes with 2.5 mM Fenton activator. (J) Various hydrogen peroxide catalysts at the cathode with various activators (2.5 mM). Carbon felt with FeOCl showed the fastest degradation of Rhodamine B, however the reusability of carbon felt is poor, and electrode replacement was need each cycle. It is also very porous, thus the absorption of solution is very high.

Figure 3. H-cell studies were used to characterize the redox reservoir (RR) and its paring with the cathodic and anodic processes. (A) Schematic illustrating the pairing of cathodic production of hydrogen peroxide with the RR anode. (B) Schematic illustrating the pairing of anodic production of persulfate with the RR cathode. (C) Plot of galvanostatic cycling measurements of the RR electrode showing the capacity (mAh/g) for charge and discharge for cycles 1-60. Galvanostatic cycling measures in 0.4 M Na_2SO_4 with pH adjusted to 3 showed an initial capacity of 82 mAh/g for charge with 97.8% capacity retention and 86 mAh/g for discharge with 93.0% capacity retention after 60 cycles at a charge/discharge rate of 1 C (C rate indicates the charge/discharge time is 60/n minutes). Inset shows a photo of an RR electrode. (D) A rate capability test in 0.4 M Na_2SO_4 (pH=3), showed excellent capacity retention of 92.6% for charge and 85.8% for discharge at a rate of 20 C, indicating that the RR can tolerate high current mismatches between the optimal conditions of hydrogen peroxide and persulfate production. (E) As evidenced by the charge and discharge capacities, there is a slight mismatch in charge and

discharge capacity for FeHCF RR that is reflected in a representative trace. Inset in (E) shows a SEM image of FeHCF materials used to fabricate the RR electrode.

Figure 4. (A) In one cycle of RR-mediated tandem oxidation treatment of PFOS, there was a 74.2% decrease in PFOS concentration observed followed by much lower decreases in concentration in subsequent cycles. This supports that a PFAS pre-concentration step is beneficial for good performance for electrochemical degradation techniques. After four cycles of degradation treatment, a 91% decrease of the original PFOS concentration (319.8 ppm) was observed. (B) The major product observed via ion chromatography was formate. For the 4 cycles of RR-mediated PFOS degradation treatment, 93.8% of the carbon balance can be attributed to formate production, meaning 85.7% of the starting PFOS was converted to formate. This corresponds to a Faradaic efficiency of 29.4%. (C) LC-MS chromatograms show different PFAS intermediates are observed and a decrease in PFOS peak that is reflected. (D) An inset of the panel shows a slight increase in PFBS (a short chain intermediate) during cycles 3 and 4 of treatment. Concentrations of PFOS were calculated by integrating the peak area corresponding to PFOS and converting this to concentration using a calibration curve. An internal standard was used to normalize the signal and compensate for instrument fluctuations. All samples were run in triplicate. Formate was quantified using ion chromatography by integrating and comparing the area of the formate peak to a calibration curve. (E) Chromatograms and (F) mass spectrometry data confirm the various PFAS intermediates observed throughout the degradation process. There is evidence of shorter chain products that double in area with a double injection volume.

Figure 5. Quantification of the fluoride ion products using ion chromatograms. (A) Only very small concentrations of free fluoride ions are observed in the RR-mediated electrochemical degradation samples. (B) This is because the FeOCl Fenton activator undergoes halide exchange with the free fluoride in solution. The crystal structure for FeOCl is shown, with green atoms corresponding to chloride that is being exchanged for free fluoride in solution. (C) Powder x-ray diffraction studies support this change from FeOCl to FeOF with the appearance of peaks at 2thetas of 27, 35, and 39 degrees not seen in the original FeOCl powder. There is still a fraction of FeOCl that is not converted, as can be seen by the much lower intensity peaks at 2thetas of 11 and 26 degrees.

Figure 6. (A) Concentrations of PFOS over multiple RR-mediated tandem oxidation cycles with various starting concentrations, hydrogen peroxide production catalysts ($NiSe_2$ or Fe-CNT),

redox reservoirs (FeHCF or NiHCF), and Fenton activator (FeOCl or zero valent iron) showing decrease in PFOS concentrations in all cases. Concentration of PFOS is quantified using LC-MS. Lower starting concentration runs passed less charge per cycle. (B) Normalized concentrations of PFOS over multiple RR-mediated tandem oxidation cycles with various starting concentrations, hydrogen peroxide production catalysts ($NiSe_2$ or Fe-CNT), redox reservoirs (FeHCF or NiHCF), and Fenton activator (FeOCl or zero valent iron) showing decrease in PFOS concentrations in all cases. Concentration of PFOS is quantified using LC-MS. Lower starting concentration runs passed less charge per cycle.

Figure 7. Plot of potential vs capacity showing the operation range of potentials for redox reservoir. The potential range of FeHCF RR is from -0.25 V to 0.65 V vs SCE. If using the full potential range of the material, there is still voltage savings of 168 mV and 160 mV compared to the thermodynamic potentials of oxygen evolution and hydrogen evolution, which are the typical counter electrode processes if the redox reservoirs are not used to do these reactions in tandem. Even higher voltage savings are expected due to the kinetic overpotentials needed to run these counter electrode reactions on catalysts.

Figure 8. (A) Example of PFOS peak integrated from the base chromatogram acquired via LC-MS for the calibration curve. (B) Calibration curve with linear fit from integrating peak for PFOS peak area averaged over three injections per calibration curve point. (C) Calibration curve with linear fit from normalizing average peak area from three injections per calibration curve point to the chloramphenicol internal standard.

Figure 9. (A) Ion chromatogram showing increase in formate peak over cycles. (B) Example of calibration curve with fit for formate and fluorine from integrating peaks from ion chromatograms of standard solutions with concentrations of 0.1 to 20 ppm.

Figure 10. A flow chart of a method for degradation of a perfluorinated or polyfluorinated alkyl substance (PFAS), according to an aspect of the disclosure.

DETAILED DESCRIPTION OF THE INVENTION

Per- and polyfluoroalkyl substances (PFAS) or "forever" chemicals are being found in increasingly widespread areas and amounts in the environment. These chemicals have been linked to numerous health problems in humans. While technologies exist for collection or separation of PFAS from water and other media, methods of complete destruction or conversion to more benign

forms of carbon and fluorine are lacking. Effective electrochemical approaches for complete, energy efficient degradation of PFAS are needed.

Disclosed herein are electrochemical cells, systems, and methods for the electrochemical degradation of PFAS using two oxidative processes in tandem over multiple cycles. The technology utilizes an electrochemical cell and electrochemical methods to cycle between the production of persulfate and hydrogen peroxide in the presence of a redox reservoir and a Fenton activator to produce sulfate and hydroxyl radicals in a sequential fashion.

As shown in FIG. 1A, the first step of the cycle is electron abstraction from the PFAS, using the specific example of PFOS. In the first step, sulfate radicals electrochemically produced by an anodic process activate the PFAS to form a PFAS radical. In the second step of the cycle, hydroxyl radicals are generated via an electrochemical cathodic process which degrade the activated perfluoroalkyl chain by one CF_2 unit. The cycle can be repeated to generate additional sulfate radicals to activate the remaining perfluoroalkyl chain and then to generate additional hydroxyl radicals to remove another CF_2 unit. Such oxidative destruction occurs cyclically, one CF_2 unit at a time. The cycle can be repeated one or more times until the PFOS chain has been converted fully or partially to degradation products. Exemplary degradation products can include formate, formic acid, CO_2, HF, and fluoride ions.

As shown in FIG. 1B, the electrochemical degradation may be performed in a single undivided cell using an anode comprising a persulfate catalyst, a cathode comprising a hydrogen peroxide catalyst, a Fenton activator, and a redox reservoir. Persulfate is produced electrochemically at the anode while the redox reservoir serves as the cathode. The produced persulfate is activated with a Fenton activator to generate the sulfate radicals for oxidizing PFAS. Then, the electrochemical bias is changed so that the redox reservoir now serves as the anode while hydrogen peroxide is formed at the cathode. Hydrogen peroxide is activated with the Fenton activator to produce hydroxyl radicals for oxidizing PFAS. This cycle of persulfate and hydrogen peroxide generation is repeated as needed to degrade PFAS completely.

The electrochemical cell shown in FIG. 1B allows for the temporal separation of the two advanced oxidative processes to avoid undesirable side reactions between the components of the two advanced oxidative processes. Additionally, the electrochemical cell as shown in FIG. 1B may avoid non-productive counter electrode reactions, such as the oxygen evolution reaction (OER). The technology uses a redox reservoir, a material that reversibly stores electrons and ions. In the

first step, the redox reservoir is reduced during the oxidation of interest where sulfate radicals are generated and utilized to oxidize PFAS to form a PFAS radical. In the second step, the redox reservoir is oxidized during the reduction of interest where hydroxyl radicals are generated and utilized to degrade the activated perfluoroalkyl chain.

These two processes, formation of sulfate radical and formation of hydroxyl radical, are not typically compatible in an undivided cell because the strong oxidants will react with each other. Using a decoupled process mediated by the RR, the two electrochemical half reactions can be carried out in the same cell but temporally separated, with high energy efficiency. The presence of the redox reservoir avoids the combination of oxidants and electrode reactions that would occur without the temporal separation. For example, as shown in FIG. 1C, H_2O_2 generated at the cathode could react at the anode, with the persulfate or sulfate radical. The hydroxyl radicals can react with the sulfate radicals. Persulfate could react at the cathode. The redox reservoir has unique properties that allow these advanced oxidative processes to be performed in the same cell, albeit temporally separated.

Per- and polyfluoroalkyl substances (PFAS)

PFAS refers to a diverse group of chemicals characterized by a fully or partly fluorinated carbon chain connected to different functional groups. PFAS are persistent and distributed ubiquitously in the global environment, biota, and humans. PFAS bioaccumulates and can cause various adverse effects in wildlife and humans. Based on the length of the fluorinated carbon chain, the PFAS may be characterized as short or long chain PFAS. In some instances, the PFAS is polymeric. In other instances, the PFAS are non-polymeric. Exemplary non-polymeric PFAS include perfluoroalkyl acids (e.g., perfluoroalkyl carboxylic acids, perfluoroalkyl sulfonic acids, perfluoroalkyl phosphonic acids, or perfluoroalkyl phosphinic acids), perfluoroalkane sulfonyl fluorides, perfluoroalkyl iodides, and per- and polyfluoroalkyl ethers. Exemplary polymeric PFAS include fluoropolymers (e.g., polytetrafluoroethylene (PTFE), polyvinylidene fluoride (PVDF), fluorinated ethylene propylene (FEP), perfluoroalkoxyl polymer (PFA), and polyvinyl fluoride (PVF)), side-chain fluorinated polymers (e.g., fluorinated (meth)acrylate polymers, fluorinated urethane polymers, and fluorinate oxetane polymer), or perfluoropolyethers. Common PFAS include perfluorooctyl carboxylic acid (PFOA) and perfluorooctyl sulfonic acid (PFOS).

PFAS can be included in the electrolyte in a concentration of between 10 ppm and 400 ppm. In some examples, PFAS can be included in the electrolyte in a concentration of between 200 ppm and 350 ppm.

The PFAS can be introduced as a contaminated feedstock into the electrochemical cell. In some examples, the contaminated feedstock can be concentrated before introduction to the electrochemical cell. In some examples, PFAS can be provided in a raw sample obtained from the environment (such as natural water body, sludges, and biosolids). Additionally, and alternatively, PFAS can be provided in a concentrated form. For example, ion exchange resins or other absorbents may be used to sequester PFAS from water and effluent from the ion exchange resins comprising concentrated PFAS may be introduced into the electrochemical cells described herein for degradation.

Redox reservoir

The electrochemical cell for degradation of PFAS as disclosed herein can include a redox reservoir. In one embodiment, the redox reservoir is a three-dimensional array of metal ions bridged by non-metal ions. In one example, the redox reservoir can be a Prussian Blue analog, or a metal hexacyanoferrate. The chemical structure of the Prussian Blue analog is characterized by the general structural formula: $A_xM_y[Fe(CN)_6]_z \cdot nH_2O$, with the specific x, y, z and n parameters and the type of monovalent cation (A = K^+, Na^+, NH_4^+), and a bivalent transition metal cation (M = Fe^{2+}, Ni^{2+}, Co^{2+}, Mn^{2+}, Cu^{2+}, Zn^{2+}, etc.) and a trivalent transition metal cation (M = Fe^{3+}, Co^{3+}, Mn^{3+}, Cr^{3+}, etc.) . In one specific example, the redox reservoir can be nickel hexacyanoferrate (NiHCF). In another specific example, the redox reservoir can be iron hexacyanoferrate (FeHCF). In a further example, the redox reservoir can be copper hexacyanoferrate (CuHCF). Any battery materials that are stable under weakly acidic to neutral pH solutions can be suitable for use as a redox reservoir, including metal oxides, MXenes, covalent organic frameworks, and liquid metals. Other materials suitable for use as the redox reservoir are disclosed in the following references, incorporated herein in their entireties: (1) Polyanionic (Phosphates, Silicates, Sulfates) Frameworks as Electrode Materials for Rechargeable Li (or Na) Batteries Christian Masquelier and Laurence Croguennec Chemical Reviews 2013 113 (8), 6552-6591 DOI: 10.1021/cr3001862; (2) Bin, D. et al. (2018) Progress in Aqueous Rechargeable Sodium-Ion Batteries. Adv. Energy

Mater. 8, 1703008; and (3) Chao D, et al. Roadmap for advanced aqueous batteries: From design of materials to applications. Sci Adv 6, eaba4098 (2020).

The redox reservoir can have a three-dimensional structure with ionic channels, where the ionic channels are interconnected cavities or pores within the three-dimensional structure. The ionic channels can have an effective diameter, or pore size, ranging between 0.3 nm to 2 nm. The ionic channels can be occupied by hydrated ions. The hydrated ions may be bound in the ionic channels by electrostatic attraction. For example, cations may be bound within an ionic channel having a negatively charged component. In another example, anions may be bound within an ionic channel having a positively charged component. The ionic channels can be large enough for the hydrated ions to exchange and move freely through the channels when the redox reservoir is in contact with a liquid solution. As an electrode, the redox reservoir can act as either an anode or a cathode.

Anode

The anode of FIG. 1B comprises a persulfate catalyst capable of oxidizing sulfate to persulfate. In one example, the persulfate catalyst can be boron doped diamond. Moreover, anodes with high potential for oxygen evolution reaction, such as glassy carbon, platinum, PbO_2, SnO_2, Ti_4O_7, TiO_2@PbO_2, could also be used for electrochemical synthesis of persulfate from sulfate.

Cathode

The cathode of FIG. 1B comprises a H_2O_2 catalyst. The H_2O_2 catalyst selectively reduces O_2 and H^+ to H_2O_2. In one example, the H_2O_2 catalyst can be iron-doped carbon nanotubes. In another example, the persulfate catalyst can be FeSe. In a further example, the hydrogen peroxide catalyst can be carbon felt. In certain examples, the hydrogen peroxide catalyst can be $NiSe_2$. The hydrogen peroxide catalyst can be any active and selective 2e oxygen reduction reaction (ORR) electrocatalyst stable in weakly acidic to neutral solution. One class is metal chalcogenides, meaning an anion from Group 16 of the periodic table and one metal element. These elements can result in various phases and exist in different stoichiometries. The chalcogenides can also be mixed cationic. The catalysts can be Fe-containing dual or single atom catalysts (Fe on nitrogen doped carbon or Fe-NC, CoFe-NC) or metal organic frameworks. Additionally, and alternatively, the H_2O_2 catalyst can be selected from the catalysts disclosed in the following references, incorporated

herin in their entireties: (1) R. Dominic Ross, Hongyuan Sheng, Yujia Ding, Aurora N. Janes, Dawei Feng, J. R. Schmidt, Carlo U. Segre, and Song Jin. Operando Elucidation of Electrocatalytic and Redox Mechanisms on a 2D Metal Organic Framework Catalyst for Efficient Electrosynthesis of Hydrogen Peroxide in Neutral Media. J. Am. Chem. Soc., 2022, 144, 34, 15485-15854. DOI: 10.1021/jacs.2c06810; (2) Hongyuan Sheng, Aurora N. Janes, R. Dominic Ross, Heike Hofstetter, Kwanpyung Lee, J. R. Schmidt & Song Jin. Linear paired electrochemical valorization of glycerol enabled by the electro-Fenton process using a stable $NiSe_2$ cathode. Nature Catalysis, 2022, 5, 716–725. DOI: 10.1038/s41929-022-00826-y; (3) Jung, E.; Shin, H.; Hooch Antink, W.; Sung, Y.-E.; Hyeon, T. Recent Advances in Electrochemical Oxygen Reduction to H_2O_2: Catalyst and Cell Design. ACS Energy Lett. 2020, 5, 1881–1892, DOI: 10.1021/acsenergylett.0c00812; (4) Hongyuan Sheng, R. Dominic Ross, J. R. Schmidt, and Song Jin. Metal-Compound-Based Electrocatalysts for Hydrogen Peroxide Electrosynthesis and the Electro-Fenton Process. ACS Energy Lett. 2023, 8, 1, 196–212. DOI: 10.1021/acsenergylett.2c01945; and (5) U.S. Application Ser. No. 18/532,418.

Fenton Activator

The Fenton activator is a part of both advanced oxidative processes. In the persulfate reaction, the Fenton activator converts persulfate to sulfate radicals. In the hydrogen peroxide reaction, hydrogen peroxide is activated with the same Fenton activator to produce hydroxyl radicals.

In one example, the Fenton activator can be zero valent Fe (Fe^0). In one example, the Fenton activator can be Fe_2O_3. In another example, the Fenton activator can be $FeSO_4$. In a further example, the Fenton activator can be FeOCl. In another example, the Fenton activator can be FeOF. In another example, the Fenton activator can be the mixed halide material $FeO(F_xCl_{1-x})$ where both F and Cl are present in the halide lattice sites. The Fenton activator can be any combination of the aforementioned. The Fenton activator can be a solid. Additionally, and alternatively, the Fenton activator can be immobilized on a substrate. Other suitable Fenton activators include Fe containing dual or single atom catalysts (e.g., Fe on nitrogen doped carbon or Fe-NC, CoFe-NC), Fe containing graphitic nitride (e.g., Fe-C_3N_4), pyrolyzed Prussian blue, Prussian blue analogues, Fe on reduced graphene oxide (rGO), and sandwiches of these catalysts (rGO-Fe-C_3N_4), and pyrite (FeS_2). Other Fenton metals that can be used as the Fenton activator

include Cu (e.g., homogeneous Cu, zero valent copper, CuO), Mn (e.g., homogeneous Mn, zero valent manganese, MnO_2 (alpha-, beta-, delta phase), other stoichiometric manganese oxides), and Co (e.g., homogeneous Co, CoO, CoS_2, Co_3S_4, Co_9S_8). Further suitable Fenton activators include Fe containing metal organic frameworks, mixed metal spinels, spinel-type oxides. Composites of these metal-containing compounds with various forms of nanostructured carbon can be used as Fenton activators.

Electrolyte

Persulfate can be activated in pH 2-11. Hydrogen peroxide can be activated in acidic to neutral conditions, however this range continues to be expanded. The electrolyte can be acidic to neutral. In some examples, the electrolyte is aqueous and can have a pH between 1 and 7. In some examples, the electrolyte is aqueous and can have a pH between 1 and 4. In some examples, the pH of the electrolyte can be between 2 and 4. In certain examples, the pH of the electrolyte can be between 2.5 and 3.5. In other examples, the pH of the electrolyte can be about 3. In some examples, the electrolyte can include sulfate, persulfate, sulfate radical and combinations thereof. In further examples, the electrolyte can include hydrogen peroxide, hydroxyl radical and combinations thereof. In other examples, the electrolyte can include formate, formic acid, CO_2, F^-, HF, Cl^-, HCl, or any combination thereof.

Electrochemical cell

The electrochemical cell includes the anode, cathode, redox reservoir, Fenton activator and electrolyte containing the PFAS. The anode and redox reservoir can be in electrical communication. The redox reservoir and the cathode can be in electrical communication at a different time. The electrochemical cell is configured to have a potential applied between either the anode and the redox reservoir or between the redox reservoir and the cathode. The electrochemical cell may be operated in batch or continuous service.

Electrochemical systems for PFAS degradation

Systems for PFAS degradation. Suitably, the electrochemical cell can be in communication with a controller. For example, the controller can be a potentiostat. At least one of the anode, cathode, and redox reservoir can be in communication with the controller. The controller can apply

the potential between the anode and the RR or between the cathode and the RR. The controller can apply a potential in response to a timer or instructions. Additionally, and alternatively, the controller can receive input from a sensor in the electrochemical cell. This tandem oxidative cycling process can be further automated, e.g., by connecting a sensor that detects the concentration of formate or other by-products and having a controller automatically adjust the cycle numbers, cycling times, potentials, the addition of more Fenton activator and supporting electrolytes, or floods in additional PFAS contaminant.

Methods of use

A flow chart of a method 100, according to an aspect of the disclosure, is shown in FIG. 10. The potential range of the redox reservoir is specific to the choice of redox reservoir material, but generally it is within the water reduction and oxidation window which is thermodynamically -0.4 to 0.8 V vs SCE. At step 110, a first electrical potential can be applied between the anode and the redox reservoir for persulfate generation. The electrochemical cell can be configured for persulfate generation without substantial oxygen evolution. At step 120, a second potential can be applied between the redox reservoir and the cathode. The first potential can be between -0.4V and +0.8V vs SCE. (SCE = saturated calomel electrode). The second potential can be between -0.4V and +0.8V vs SCE. In some examples, the first potential and the second potential can be between -0.3V and +0.4V vs SCE. In other examples, the first potential and the second potential can be between -0.2V and +0.4V vs SCE. In further examples, the first potential and the second potential can be between -0.2V and +0.2V vs SCE. Using this potential range allows the process of PFAS degradation to be energy efficient. The potential range of the BDD anode is about 2.6 V to 3.8 V vs SCE. The potential range of the $NiSe_2$ cathode is about 0.5 v to 0.65 V vs RHE (reversible hydrogen electrode).

In one example, less than 50% of charge passed results in oxygen evolution. In another example, less than 60% of charge passed results in oxygen evolution. In a further example, less than 70% of charge passed results in oxygen evolution. In some examples, less than 80% of charge passed results in oxygen evolution. In other examples, less than 90% of charge passed results in oxygen evolution. In a still further example, less than 95% of charge passed results in oxygen evolution.

In one example, the electrochemical cell is configured for Faradaic efficiency greater than 5%. In another example, the electrochemical cell is configured for Faradaic efficiency greater than 10%. In a further example, the electrochemical cell is configured for Faradaic efficiency greater than 15%. In certain examples, the electrochemical cell is configured for Faradaic efficiency greater than 20%. In other examples, the electrochemical cell is configured for Faradaic efficiency greater than 25%.

The first potential may be applied for a first application time at step 110 and the second potential may be applied for a second application time at step 120. In some cases, application of the first potential for the first application time and application of the second potential for the second application time is repeated for one or more cycles as in step 130. The first application time should be different than the second application time. For example, the first application time and the second application time may alternate without any intervening temporal gaps or overlap. In other cases, there may be temporal gaps between the first application time and the second application. In yet other cases, there may be temporal overlap between the first application time and the second application so long as the first application time and second application are not completely overlapping. By way of example for illustration purposes only, a one-hour cycle may include a first application time for 40 minutes and the second application time for 20 minutes of the one-hour cycle. By way of another example, a one-hour cycle may include a first application time for the first 35 minutes, a 5-minute gap without application of the first or second potential, a second application time for 18 minutes, and another 2 minutes without application of the first or second potential of the one-hour cycle. By way of yet another example, a one-hour cycle may include a first application time for 41 minutes and the second application time for the second 21 minutes of the one-hour cycle, thereby having time where the first potential and the second potential are applied at the same time.

The duration of the cycle may be 1-100% of the full charge and discharge of the redox reservoir (state of charge, SOC).

The duration of persulfate production may be 1-100% of the charge stored by the redox reservoir (state of charge, SOC).

The duration of hydrogen peroxide production may be 1-100% of the charge stored by the redox reservoir (state of charge, SOC).

The redox reservoir has a capacity, or a capability to store and release an amount of charge. The cycle can be controlled by the storge and release of charge. In some examples, the cycles can be controlled by the time passed. In other examples, the cycles can be controlled by the amount of charge passed.

In some examples, a pre-cycle preparation step is performed with the redox reservoir at step 105. The pre-cycle preparation step includes 1-4 cycles of applied potential until the capacity of the redox reservoir stabilizes. The stabilization can be defined by a capacity retention of at least 90% for charge at a charge/discharge rate of 1 C, after cycling the applied potential. This activation step ends at setting the redox reservoir at a potential to begin the persulfate production step. For example, when the redox reservoir is an FeHCF electrode, the potential is set to 0 V vs Hg/Hg_2SO_4 electrode before beginning the PFAS degradation treatment.

In some cases, the methods may further comprise recovering fluoride ion at step 140 after PFAS degradation. As demonstrated in the Examples, certain Fenton activators, such as FeOCl, may undergo halide exchange. This advantageously allows for sequestering fluoride ion (e.g., as FeOF) to recover fluoride, which is more stringently controlled in drinking water than the liberated chloride ion.

Miscellaneous

Unless otherwise specified or indicated by context, the terms “a”, “an”, and “the” mean “one or more.” For example, “a molecule” should be interpreted to mean “one or more molecules.”

As used herein, “about”, “approximately,” “substantially,” and “significantly” will be understood by persons of ordinary skill in the art and will vary to some extent on the context in which they are used. If there are uses of the term which are not clear to persons of ordinary skill in the art given the context in which it is used, “about” and “approximately” will mean plus or minus $\leq$10% of the particular term and “substantially” and “significantly” will mean plus or minus >10% of the particular term.

As used herein, the terms “include” and “including” have the same meaning as the terms “comprise” and “comprising.” The terms “comprise” and “comprising” should be interpreted as being “open” transitional terms that permit the inclusion of additional components further to those components recited in the claims. The terms “consist” and “consisting of” should be interpreted as being “closed” transitional terms that do not permit the inclusion additional components other than

the components recited in the claims. The term "consisting essentially of" should be interpreted to be partially closed and allowing the inclusion only of additional components that do not fundamentally alter the nature of the claimed subject matter.

All methods described herein can be performed in any suitable order unless otherwise indicated herein or otherwise clearly contradicted by context. The use of any and all examples, or exemplary language (e.g., "such as") provided herein, is intended merely to better illuminate the invention and does not pose a limitation on the scope of the invention unless otherwise claimed. No language in the specification should be construed as indicating any non-claimed element as essential to the practice of the invention.

All references, including publications, patent applications, and patents, cited herein are hereby incorporated by reference to the same extent as if each reference were individually and specifically indicated to be incorporated by reference and were set forth in its entirety herein.

Preferred aspects of this invention are described herein, including the best mode known to the inventors for carrying out the invention. Variations of those preferred aspects may become apparent to those of ordinary skill in the art upon reading the foregoing description. The inventors expect a person having ordinary skill in the art to employ such variations as appropriate, and the inventors intend for the invention to be practiced otherwise than as specifically described herein. Accordingly, this invention includes all modifications and equivalents of the subject matter recited in the claims appended hereto as permitted by applicable law. Moreover, any combination of the above-described elements in all possible variations thereof is encompassed by the invention unless otherwise indicated herein or otherwise clearly contradicted by context.

EXAMPLES

Example 1:

The present Example demonstrates electrochemical reaction (FIG. 1A) for the degradation of PFAS using a redox reservoir, an anode, a cathode, and a Fenton activator (FIG. 1B). The two most common advanced oxidation processes are the activation of hydrogen peroxide via metal cations to more potent hydroxyl radicals, known as the Fenton process, or of persulfate to sulfate radicals. When hydrogen peroxide is produced electrochemically via the 2-electron reduction of oxygen, this is termed the electro-Fenton process. It is known that PFOA is more susceptible to degradation by hydroxyl radicals than PFOS. There are previous reports for PFOA degradation via

the electro-Fenton process with oxygen evolution and direct oxidation occurring at the counter electrode. The sulfonate head group of PFOS is more electron withdrawing, resulting in the electron abstraction step from the head group being more difficult and rendering hydroxyl radicals ineffective. Hydroxyl radicals are generally less selective, and can perform hydrogen atom transfer and electron abstraction, while sulfate radicals are more selective and prefer electron abstraction. However, electron abstraction processes on their own are also insufficient for complete degradation of PFAS, because the overproduction of persulfate radicals potentially results in the sulfonate group being re-introduced to the activated perfluoroalkyl chain.

Herein is disclosed an electrochemical system to cycle between the production of persulfate and hydrogen peroxide electrochemically in the presence of a Fenton activator to produce sulfate and hydroxyl radicals. Sulfate radicals activate the PFAS and then hydroxyl radicals degrade the activated chain, avoiding the excess production of radicals meant for degradation. Therefore, the oxidative destruction of PFAS occurs cyclically, one CF_2 unit at a time, requiring continuous activation of the perfluoroalkyl chain. Such tandem and cyclic oxidation process ensures the effective and complete degradation of PFAS, including the most challenging PFOS, into formate and fluoride ions. This unique electrochemical set-up also avoids non-productive counter electrode reactions, such as the oxygen evolution reaction, and allows for the temporal separation of these two advanced oxidative processes to avoid side reactions. This is possible by using a “redox reservoir” (RR), a material that reversibly and temporarily stores electrons and ions. The RR is reduced during the oxidation of interest, then oxidized during the reduction of interest. These two processes are not typically compatible in an undivided cell because the strong oxidants will react with each other. Using a decoupled process mediated by the RR electrode, we are able to temporally separate the two electrochemical half reactions in the same cell with high energy efficiency. With this technique, 86% degradation of 350 ppm PFOS to formate and fluoride ions with approximately 29.4% Faradaic efficiency (confirmed via liquid chromatography tandem mass spectrometry and ion chromatography) was achieved.

Results and Discussion

Investigation of Electrochemical Production and In-Situ Activation of Hydrogen Peroxide and Persulfate

Boron-doped diamond (BDD) films may be used for persulfate production and have low catalytic activity for oxygen evolution, the predominant competition reaction at high oxidation potentials. Sulfate anions from the electrolyte are used to produce persulfate. Increasing the concentration of sulfate anions present led to increased Faradaic efficiency for persulfate production, quantified with iodometric detection. However, high salt concentrations are detrimental for mass spectrometry analysis, therefore the lowest concentration that resulted in reasonable persulfate production was selected. A plateau was observed from 0.4 to 0.5 M, therefore 0.4 M Na_2SO_4 was used moving forward. An optimal potential of 2.78 V vs SCE was determined for persulfate production for 0.4 M Na_2SO_4 with pH adjusted to 3, because this is the desirable optimal pH for Fe-mediated electro-Fenton process and persulfate activation can be achieved over a wider pH range of approximately 2-11. Constant-potential bulk electrosynthesis measurements in Argon purged 0.4 M Na_2SO_4 with pH adjusted to 3 were conducted in a two-compartment H-cell, which showed an increasing Faradaic efficiency as more charged is passed with a value of 43-44% when over 10C of charge is passed, resulting in a concentration of 300 ppm. PFOS oxidation can also occur at high oxidation potentials, but this is not considered a competing reaction because it would also cause direct electron transfer from PFAS. However, persulfate production and direct PFOS oxidation occur at similar potentials, therefore persulfate production in the presence of 350 ppm PFOS was studied. It was found that a higher potential was needed for persulfate production than in solutions not containing PFOS, with the optimal potential being 3.3 V. This corresponds to a current of 8-12 mA. The Faradaic efficiencies were lower at these conditions, potentially due to increased competition with oxygen evolution as well as PFOS oxidation. Constant current studies resulted in higher Faradaic efficiencies as more charge was passed.

To study persulfate activation, 40 ppm Rhodamine B (RhB) solution was used as a model system. Degradation tests were conducted in Ar-purged 0.4 M Na_2SO_4 adjusted to pH 3 with H_2SO_4 and 2.5 mM Fe activator in an H cell separated by a glass frit. The BDD anode was operated at 2.78 V vs SCE to enable efficient persulfate production. UV-vis spectrophotometry was used to monitor the decrease in RhB concentration over time. The current remained stable over time, indicating it was not direct oxidation resulting in this decrease. Among the different activators studied, FeOCl showed much faster degradation than $FeSO_4$, with almost complete degradation after 60 minutes, compared to a 45% decrease in RhB concentration with homogenous $FeSO_4$.

Commonly, carbon based electrodes are used for hydrogen peroxide production. However, their performance in acidic conditions is often lower than neutral to alkaline conditions. $NiSe_2$ can serve as a high performing acidic 2e-ORR catalyst with selectivity and excellent stability against surface oxidative leaching in the presence of hydrogen peroxide and hydroxyl radicals. Constant-potential bulk electrosynthesis measurements in O_2 saturated 0.4 M Na_2SO_4 with pH adjusted to 3 conducted in a two-compartment H-cell allowed the production of H_2O_2 up to a concentration of 150 ppm with a consistent Faradaic efficiency of 45-46%. With increasing accumulation of H_2O_2, reduction can occur at the $NiSe_2$ electrode. However, high accumulation of H_2O_2 is not needed due to its immediate in-situ activation into hydroxyl radicals for degradation of PFOS. Similarly for the persulfate production and activation, a 40 ppm RhB solution in 0.4 M Na_2SO_4 with pH adjusted to 3 containing 2.5 mM of Fenton activator was used to study the radical production capacity of the BDD electrode. When comparing the activation of hydrogen peroxide with FeOCl and $FeSO_4$, the performance is very similar with complete degradation of RhB after 30 minutes of HPR and both are suitable Fenton activators.

Modular Production of Persulfate and Hydrogen Peroxide without PFOS Present

To achieve the paired production of these two oxidants, a suitable redox reservoir material should be selected. This redox reservoir material should have fast redox kinetics, high stability, and high charge-storage capacity in the electrolyte of interest. Iron hexacyanoferrate, or Prussian Blue, was selected to pair the half reactions. Prussian blue was synthesized via the single-iron source method and resulted in micro-meter sized cubes. The powder X-ray diffraction pattern corresponds to the cubic phase (JCPDS no. 52-1907). Galvanostatic cycling measurements in 0.4 M Na_2SO_4 with pH adjusted to 3 showed an initial capacity of 82 mAh/g for charge with 97.8 % capacity retention after 60 cycles and 86 mAh/g for discharge with 93.0% capacity retention after 60 cycles at a charge/discharge rate of 1 C (C rate indicates the charge/discharge time is 60/n minutes). A rate capability test in 0.4 M Na_2SO_4 (pH=3), showed excellent capacity retention of 92.6% for charge and 85.8% for discharge at a rate of 20 C, indicating that the RR can tolerate high current mismatches between the optimal conditions of hydrogen peroxide and persulfate production.

To study the production of oxidants with the FeHCF RR, each reaction was run in separate undivided cells. For hydrogen peroxide production, a $NiSe_2$ cathode was used at a constant

potential yielding an approximate final concentration of 40 ppm. When the oxidation of FeHCF RR was paired, the Faradaic efficiency (85%) was even higher than the FE (46%) in the typical H-cell configuration using oxygen evolution as the counter electrode process. For persulfate production, a BDD cathode was run at constant potential yielding an approximate final concentration of 140-180 ppm, when the reduction of the FeHCF RR was paired. The Faradaic efficiencies were on par with what was seen using an H-cell configuration with hydrogen evolution as the counter electrode reaction, at approximately 43%.

Degradation performance of RR-mediated system

Evaluating the degradation products of PFAS degradation systems allows for evaluating PFAS mitigation strategies. Due to the low concentrations of PFAS, liquid chromatography mass spectrometry (LC-MS) must be used to monitor the decrease in PFOS as well as any increases in intermediate PFAS species. Shorter chain intermediates are believed to be harder to degrade due to the decreasing electron affinity, therefore their concentrations are closely monitored. For inorganic and lower mass organic anions, ion chromatography can be used for quantification.

In one cycle of RR-mediated PFOS oxidation treatment, there is a 74.2% decrease in PFOS followed by much lower decreases in PFOS concentration in subsequent cycles (FIG. 4). This supports that a pre-concentration step is helpful for good performance for electrochemical techniques. After four cycles of oxidation treatment, a 91% concentration decrease in PFOS (319.8 ppm) is observed. In comparison, when adding 1.75 mM of persulfate and hydrogen peroxide by chemical addition with activator only resulted in a 42.9% concentration decrease after one cycle. After 4 cycles of this chemical and activator addition, only a 52% decrease in PFOS was observed. When increasing the per cycle concentration of oxidants to 3.5 mM, a very similar concentration decrease of 41.4% was observed for one cycle.

The major product observed via ion chromatography after the oxidation treatment cycles was formate. For the 4 cycles of RR-mediated oxidation treatment, 93.8% of the carbon balance can be attributed to formate production, meaning 85.7% of starting PFOS was converted to formate. This corresponds to an energy efficiency of 29.4%.

Fluoride ions can also be quantified based on the ion chromatograms (FIG. 5). However, only very small concentrations of free fluoride are observed in the RR-mediated electrochemical degradation samples. This is because the FeOCl Fenton activator undergoes halide exchange with

the free fluoride in solution. Powder x-ray diffraction studies support this change from FeOCl to FeOF with the appearance of peaks at 2thetas of 27, 35, and 39 degrees not seen in the original FeOCl powder. There is still a fraction of FeOCl that is not converted, as can be seen by the much lower intensity peaks at 2thetas of 11 and 26 degrees.

After regeneration from various adsorption technologies, the resulting concentrations of PFAS are commonly on the order of hundreds of ppm. Therefore, a variety of starting PFOS concentrations were tested (FIG. 6). Both Fe-CNT and $NiSe_2$ hydrogen peroxide catalysts were tested together with NiHCF and FeHCF redox reservoirs, and FeOCl and zero valent Fe Fenton activators. Higher PFOS starting concentrations were favorable for degradation efficiency, likely because a higher bulk concentration enhances mass transfer to the electrode surface and increases the likelihood that the PFAS will interact with the radical species. If the hydrogen peroxide catalyst was directly paired with the persulfate production catalyst, the oxidative species would interfere and further lower the efficiency. If these two oxidative processes are run in tandem with typical counter electrode processes, the incorporation of catalysts for hydrogen evolution (HER) and oxygen evolution (OER) would be required. The potential range of FeHCF is -0.25 V to 0.65 V vs SCE. If using the full potential range of the material, there is still voltage savings of 168 mV and 160 mV compared to the thermodynamic potentials of OER and HER (FIG. 7). There are even higher voltage savings expected due to the kinetic overpotentials needed to run these counter electrode reactions on catalysts. Also, the more reductive and oxidative the potentials are, the higher the likelihood of degradation of products at the electrode. Therefore, running the tandem oxidation treatment mediated using a redox reservoir results in energy savings. Considering the scale of PFAS contamination and treatment needed, it is important to enhance the energy efficiency and lower the operational cost of the degradation technologies.

Methods

RR-mediated degradation of PFOS

30 mL of 350 ppm PFOS in 0.4 M Na_2SO_4 (pH=3) was added to a 50 mL polypropylene beaker with 20.5 mg of FeOCl. A custom made Teflon cap was used to hold 4 electrodes: 2 back to back 4 cm^2 $NiSe_2$ on CFP electrodes, a 2 cm^2 BDD electrode, an SCE reference electrode, and 4 stacked 4 cm^2 FeHCF on stainless steel mesh electrodes (active material loading of ~250 mg). This system was parafilmed to aid gas saturation for hydrogen peroxide production. The system is

first argon purged then persulfate production is run using a constant current of 12 mA while the RR is being reduced. The working electrode is the BDD electrode and the counter electrode is the redox reservoir. Then, the system is saturated with oxygen gas and hydrogen peroxide production is run using a constant potential of 0.6 V vs RHE while the RR is being oxidized. The working electrode is the $NiSe_2$ electrode and the counter electrode is the redox reservoir. This is repeated for multiple cycles of treatment. Equal amounts of charge were passed for each half-reaction. The maximum charge passed per cycle was 16.2 Coulombs. The cycle length is only limited by the capacity of the redox reservoir. During these cycles, the RR electrode's potential was also monitored to prevent over-oxidation or reduction.

Conditions tested include:

Fenton activators: zero valent Fe. Fe_2O_3, $FeSO_4$, FeOCl

H_2O_2 catalysts: Fe-CNT (carbon nanotubes), FeSe, carbon felt, $NiSe_2$

Redox reservoirs: Nickel hexacyanoferrate, Iron hexacyanoferrate

Persulfate catalyst: Boron doped diamond

Synthesis of FeHCF:

0.04 M $Na_4Fe(CN)_6$ was added to a round bottom flask. While stirring at 1000 rpm, 37% HCl was added dropwise to the flask at room temperature to a concentration of 0.3 M. After adding acid, the solution was allowed to sit for 3 days at room temperature. Then, the solution was stirred at 1000 rpm at 60°C for 44 hours.

Synthesis of $NiSe_2$ catalyst on Carbon Fiber Paper (CFP):

Teflon-coated carbon fiber paper (Fuel Cell Earth, TGP-H-060) was plasma cleaned at 150 W for 5 minutes then annealed in air at 700°C for 5 min per side. A 3x6 cm^2 piece was placed in 2.1 mmol $Ni(NO_3)$, 4.2 mmol of NH_4F, and 10.5 mmol urea in 100 mL of water, and heated at 110°C for 5 hours in a 125 mL autoclave to synthesize $Ni(OH)_2$ on CFP. For the selenization step, a solution was prepared by heating 4.29 g of NaOH and 471 mg of Se power in 50 mL of water at 220°C for 24 hours in a 80 mL autoclave. The $Ni(OH)_2$ on CFP was then added to the autoclave with an additional 20 mL of water and heated at 180°C for 24 hours in the same 80 mL autoclave. The converted $NiSe_2$ on CFP was washed of excess Se using 1.25 M Na_2S in water, water, and

ethanol. The areal loading was determined by the mass change of the CFP after synthesis. All samples were used shortly after synthesis to minimize oxidation.

FeOCl synthesis:

FeOCl was synthesized by heating $FeCl_3$ powder at a ramp rate of 10°C/min to a set point of 220°C for 2 hours in an alumina crucible.

Fabrication of Redox Reservoir Electrodes:

The RR electrodes were prepared using a conventional slurry-casting method. Typically, FeHCF powder (70 wt%) and super P conductive carbon (18 wt%) were ground with a mortar and pestle for 30 min then stirred with SWCNT (2 wt%), and polyvinylidene fluoride (PVDF) (10 wt%) from TUBALL BATT NMP (consisted of 0.4 wt % SWCNT, 2 wt % polyvinylidene fluoride, > 96.7 wt % N-Methyl-2-pyrrolidone) at 800 rpm overnight at room temperature into a well dispersed slurry. This slurry was cast onto a 316 SS mesh current collector. The prepared electrodes were dried in a vacuum oven at 60°C for 12 h to remove the residual solvent. The mass loading of active material was approximately 10-15 mg cm^{-2}.

Materials Characterization:

The size and morphology of the NiHCF product were characterized using a scanning electron microscope (SEM, Zeiss SUPRA 55VP Scanning Electron Microscope) equipped with an energy dispersive X-ray spectroscopy (EDS) detector. Powder X-ray diffraction (PXRD) patterns were collected on a Bruker D8 Advance X-ray diffractometer with Cu-Ka radiation.

Solution Characterization:

Solid Phase Extraction (SPE) procedure:

Oasis WAX 6 cc/150 mg sorbent cartridges were used to remove supporting electrolyte from samples before loading onto the LC-MS. The procedure was as follows: first, 0.66 mL of methanol, 0.1% NH_4OH in methanol, and water were loaded onto the cartridge. Then, the sample was pulled under vacuum followed by 3 wash steps with 0.66 mL of water. The cartridges were dried for 10 minutes under vacuum. Then, the samples were eluted using 0.33 mL of methanol and 0.33 mL of 5% NH_4OH in 60:40 ACN:MeOH. Samples were then speed vacuumed with no heat

until dry and reconstituted to the original sample volume with 5 mM $NH_4C_2O_2H_3$ in methanol with 25 ppm chloramphenicol as an internal standard.

LC-MS procedure:

LC-MS analysis was performed using a NanoAcquity ultra-high pressure LC system (Waters, Milford, MA, USA) coupled to a high-resolution Impact II quadrupole time-of-flight (Q-TOF) mass spectrometer (Bruker Daltonics, Bremen, Germany). PFAS samples after SPE were separated through reverse-phase LC-MS on a Agilent C18 ZORBAX RRHD Eclipse Plus C18, 95Å, 2.1 x 50 mm, 1.8 µm, 1200 bar column using a 16-min gradient of 50% to 95% mobile phase B (mobile phase A: 5mM NH4OAc in water; mobile phase B: 5mM NH4OAc in 5% water 95% MeOH) at a constant flow rate of 50µL/min to acquire MS and MS/MS spectra. Data was analyzed using Bruker DataAnalysis v 4.3.

Quantification using LC-MS:

To generate a PFOS concentration calibration curve, PFOS standards were injected (2uL) in triplicate. For some data collections, 10 ppm chloramphenicol (CA) was added to the samples. Extracted ion chromatograms for PFOS (498.9 m/z) and CA (321.0 m/z) were generated and PFOS peak area (Figure 8A) was normalized against CA peak area if used. This value was plotted against known concentrations to generate a linear response curve used to determine unknown PFOS concentrations (Figure 8B and 8C). PFAS species ID's were confirmed through retention time, accurate mass measurements and targeted MS/MS. Examples of PFOS peaks integrated from the base chromatogram acquired via LC-MS for the calibration curve is shown in FIG. 8A. The two peaks correspond to two branched isomers of PFOS. The resulting calibration curve with linear fit from integrating peak for PFOS peak area averaged over three injections per calibration curve point is shown in FIG. 8B. There is a linear low concentration regime and high concentration regime. The resulting calibration curve with linear fit from normalizing average peak area from three injections per calibration curve point to the chloramphenicol internal standard is shown in FIG. 8C.

Ion chromatography:

The concentrations of anions in the post treatment samples were analyzed using Dionex ICS-2100 ion chromatography systems equipped with a conductivity detector and a Dionex IonPac AG/AS-14 column. A 0.8 mM Na_2CO_3 and 0.25 mM $NaHCO_3$ mobile phase was used with a flow rate of 1.2 mL/min. The current of the suppressor was 24 mA

Quantification using ion chromatography:

The standard anion solutions were prepared by dissolving NaHCOO, NaF, and NaCl in water. A calibration curve was constructed for each anion to quantify the sample solutions. Samples were prepared by diluting the post treatment solution by 100-200x. The expected concentration of formate was calculated by accounting for the dilution of the sample and comparing the molar ratios. For example, starting with 350 ppm PFOS then is 0.7 mM. 0.7 mM* 8 moles carbon/1 mole PFOS = 5.6 mM C if all PFOS is converted to formate. Then, the resulting concentration based on peak area of the ion chromatogram was used to calculate the carbon balance. For 4 cycles of treatment, the resulting concentration was 4.8 mm C. 4.8 mM C/5.6 mM C=85.7%. When considering 91.3% of the PFOS was degraded the concentration of C expected is 0.6396 mM* 8 moles carbon/1 mole PFOS = 5.1 mM C which results in a C balance of 93.8%.

$$\text{FE}\ (\%) = \frac{\text{Q for formate production}}{Q_{input}} \times 100 = \frac{[\text{formate}] \times V \times 2 \times 96485}{Q_{input}} \times 100 \qquad \text{Eq.1}$$

where V, [formate], and Q_{input} are the volume of the solution, the concentration of produced formate and the input charge during the electrosynthesis, respectively.

An example ion chromatogram showing increase in formate peak over cycles is shown in FIG. 9A. An example of a calibration curve with fit for formate and fluorine from integrating peaks from ion chromatograms of standard solutions with concentrations of 0.1 to 20 ppm is shown in FIG. 9B.

Electrochemical characterization:

All electrochemical measurements were carried out using a Bio-Logic SP-200 potentiostat, a Bio-Logic VMP-3 multichannel potentiostat, or a Bio-Logic BP-300 potentiostat. A three-

electrode cell was used for measurements with a Pt counter electrode and a reference electrode: SCE or Hg/ Hg_2SO_4.

H_2O_2 production and detection:

H_2O_2 production reaction was optimized in an H-cell with a Nafion 212 membrane with a 1 cm^2 $NiSe_2$ on CFP as the working electrode, a Pt wire, Au mesh, or graphite rod as the counter electrode, and a Hg/ Hg_2SO_4 reference electrode in 0.4 M Na_2SO_4 solution adjusted to pH 3 with 1 M H_2SO_4. Prior to the measurements, the electrolyte was purged with O_2 gas for 15 min. Cyclic voltammetry (CV) was conducted with no O_2 gas bubbling at 100 mV/s. Chronoamperometry (CA) was conducted at 0.6 V vs RHE. All potentials measured against Hg/Hg_2SO_4electrode were converted to the reversible hydrogen electrode (RHE) scale using $E_{RHE} = E_{Hg/Hg_2SO_4} + 0.640\ V + 0.059 \times pH$, where the pH values of solutions were determined using an Orion 810 BNUWP ROSS Ultra pH meter.

Detection of hydrogen peroxide

As shown in FIG. 2 (G-J), H-cell studies were used to optimize hydrogen peroxide production. (G-J) A 3-electrode set up is used with: 1 cm^2 $NiSe_2$ cathode, Pt wire anode, Hg/ Hg_2SO_4 reference electrode. 3.5 mL of electrolyte was present in the cathode compartment, 7 mL 0.05 M H_2SO_4 was present in the anode compartment. In the cathode compartment, 0.4 M Na_2SO_4 pH=3 was used for accumulation tests. For Fenton activator tests, 40 ppm of O_2 saturated RhB solution in 0.4 M Na_2SO_4 (pH=3) was used.

To determine the Faradaic efficiency (FE) of the hydrogen peroxide production, the concentration of the H_2O_2 generated from chronoamperometry (CA) was quantified by colorimetric titration with ceric sulfate. A 4 mM $Ce(SO_4)_2$ solution was prepared by dissolving $Ce(SO_4)_2$ in 0.5 M H_2SO_4 and diluted to 0.4 mM. A calibration curve was constructed with every dilution by measuring the UV-Vis spectroscopy of $Ce(SO_4)_2$ solutions using a Cary 50 SCAN spectrometer with different concentrations at a wavelength of 319 nm.

An appropriate volume of sample solution containing the produced H_2O_2 was added into 5.0 mL 0.4 mM $Ce(SO_4)_2$ solution and measured by the UV-Vis spectroscopy to determine the concentration of Ce^{4+}. The concentration of H_2O_2 could be determined by the following equations:

$$2Ce^{4+} + H_2O_2 \rightarrow 2Ce^{3+} + 2H^+ + O_2 \quad \text{Eq. 2}$$

$$[H_2O_2](mM) = \frac{V_{before} * [Ce^{4+}_{before}] - (V_{before} + \Delta V) * [Ce^{4+}_{after}]}{\Delta V * 2} \quad \text{Eq. 3}$$

where V_{before} is the original volume of the 0.4 mM Ce^{4+} solution, $[Ce^{4+}_{before}]$ and $[Ce^{4+}_{after}]$ are the concentrations of Ce^{4+} before and after adding the H_2O_2 solution, and ΔV is the amount of H_2O_2 added to solution. Then, the Faradaic efficiency can be found by comparing these concentrations according to the equation:

$$FE\ (\%) = \frac{Q \text{ for } H_2O_2 \text{ production}}{Q_{input}} \times 100 = \frac{[H_2O_2] \times V \times 2 \times 96485}{Q_{input}} \times 100 \quad \text{Eq. 4}$$

where V, $[H_2O_2]$, and Q_{input} are the volume of the solution, the concentration of produced H_2O_2 and the input charge during the electrosynthesis, respectively.

$S_2O_8^{2-}$ production and detection:

BDD film with a thickness of 1 mm (resistivity <0.1 ohm-cm) on p type (100) silicon (resistivity of 0.01–0.02 ohm-cm) wafer (Lightning 25 DoSi wafer, Advanced Diamond Technologies Inc.) was used to fabricate the anode used for persulfate production. The Si side of the DoSi wafer was etched using 24 wt % hydrofluoric acid to remove the silicon oxide, then an ohmic contact was made by attaching a piece of Cu foil and Cu tape onto the back side of the DoSi wafer with gallium-indium eutectic. The whole ohmic contact area was sealed with epoxy resin (Loctite, EA9460). The electrochemical measurements were performed with a three-electrode configuration, using a platinum wire counter electrode and an SCE reference electrode. The electrochemical impedance spectroscopy (EIS) analysis was carried out with a frequency range of 100 kHz or 200 kHz to 100 mHz at open circuit potential to check the uncompensated resistance of the electrochemical system, which was measured to be 3–6.5 ohms. CA was then carried out using both constant current and constant potential for cumulative persulfate production.

As shown in FIG. 2 (A-F), H-cell studies were performed to optimize persulfate production. A 3 electrode set up is used with: 2 cm^2 BDD anode, Pt wire cathode, SCE reference electrode. 12 mL of electrolyte are present in each compartment. Same electrolyte is used in each

compartment except for Fenton activator tests. For Fenton activator tests, 40 ppm of RhB solution in 0.4 M Na_2SO_4 (pH=3) was used in the BDD compartment only.

Detection of persulfate

To determine the Faradaic efficiency (FE) of the persulfate production, the concentration of the S_2O_8 generated from chronoamperometry (CA) was quantified by iodometric titration. An appropriate volume of sample solution containing the produced S_2O_8 was added into 5.0 mL of solution containing sodium bicarbonate and sodium iodide and measured by the UV-Vis spectroscopy at 352 nm using a Cary 50 SCAN spectrometer. A calibration curve was constructed using known concentrations of potassium persulfate. With increasing concentrations of persulfate, the solution had a darker yellow color according to the equation:

$$2I^- + S_2O_8{}^{2-} \rightarrow 2SO_4{}^{2-} + I_2 \qquad \text{Eq. 5}$$

The Faradaic efficiency was calculated by the following equation:

$$FE\ (\%) = \frac{Q \text{ for } S_2O_8 \text{ production}}{Q_{input}} \times 100 = \frac{[S_2O_8] \times V \times 2 \times 96485}{Q_{input}} \times 100 \qquad \text{Eq. 6}$$

where V, $[S_2O_8]$, and Q_{input} are the volume of the solution, the concentration of produced S_2O_8 and the input charge during the electrosynthesis, respectively.

Degradation of Rhodamine B studies for testing Fenton activators:

Degradation tests were conducted in a two-compartment three-electrode H-cells using 40 ppm rhodamine B (RhB) (≥95%) as a model organic pollutant. For persulfate production, a 2 cm^2 BDD anode operated at constant potential (2.78 V vs SCE), Pt wire cathode, and SCE reference electrode were used. 12 mL of electrolyte was present in each compartment. For hydrogen peroxide production, a 1 cm^2 $NiSe_2$ cathode operated at a constant potential of 0.6 V vs RHE, Pt wire anode, and $Hg/HgSO_4$ reference electrode were used. 3.5 mL of O_2 saturated 40 ppm RhB in 0.4 M Na_2SO_4 pH=3 electrolyte was present in the cathode compartment, 7 mL of 0.05 M H_2SO in the right compartment. During each degradation test, a small aliquot of electrolyte solution was sampled periodically from the working electrode compartment and quantitatively diluted with a

stock solution of 0.4 M Na_2SO_4 pH=3 electrolyte for UV-vis spectrophotometric determination of the organic dye concentration at 550 nm.

Electrochemical characterization of the redox reservoir:

As shown in FIG. 3, H-cell studies were used to characterize the RR. A 3-electrode set up is used with: 1 cm^2 FeHCF working electrode, Pt wire anode, SCE reference electrode. 12 mL of 0.4 M Na_2SO_4 pH=3 was present in both compartments. For studies testing RR integration, an undivided cell was used containing 0.4 M Na_2SO_4 pH=3. FIG 3A: For hydrogen peroxide production, a volume of 3.5 mL was used. FIG 3B: For persulfate production, a volume of 30 mL was used.

Table 1. Testing RR integration with hydrogen peroxide production.

Run	Deviation from above	Charge passed (C)	Faradaic Efficiency (%)
1	None	1.152	87.7
2	None	1.152	98.5
3	None	1.152	
4	Pt CE, divided cell	1.152	46.6

New solution used per run. Same electrodes used for all runs. Undivided cell configuration unless otherwise noted.

Table 2. Testing RR integration with persulfate production.

Run	Deviation from above	Charge passed (C)	Faradaic Efficiency (%)
1	None	11.8	41.1
2	None	11.8	37.3
3	None	11.8	46.3
4	Pt CE, divided cell	11.8	42.8

New solution used per run. Same electrodes used for all runs. Undivided cell configuration unless otherwise noted.

CLAIMS

1. An electrochemical cell comprising:

(a) an anode comprising a persulfate catalyst,

(b) a cathode comprising a hydrogen peroxide catalyst,

(c) a redox reservoir,

(d) a Fenton activator, and

(e) an acidic to neutral electrolyte having sulfate and at least one perfluorinated or polyfluorinated alkyl substance (PFAS) therein,

wherein the anode and redox reservoir are in electrical communication and the redox reservoir and the cathode are in electrical communication, and

wherein the electrochemical cell is configured to have a first potential applied between the anode and the redox reservoir for a first application time and a second potential applied to the redox reservoir and the cathode for a second application time that is different from the first application time.

2. The electrochemical cell of claim 1, wherein the electrochemical cell is configured to cycle application of the first potential between the anode and the redox reservoir for the first application time and application of the second potential between the redox reservoir and the cathode for the second application time.

3. The electrochemical cell of claim 1 or 2, wherein the potential is between -0.2 and 0.7 V vs SCE.

4. The electrochemical cell of any one of claims 1-3, wherein the anode comprises boron doped diamond, glassy carbon, platinum, PbO_2, SnO_2, Ti_4O_7, or TiO_2@PbO_2.

5. The electrochemical cell of any one of claims 1-4, wherein the cathode is selected from $NiSe_2$, Fe-doped carbon nanotubes, carbon felt, FeSe, and combinations thereof.

6. The electrochemical cell of any one of claims 1-5, wherein the redox reservoir is selected from one or more of nickel hexacyanoferrate and iron hexacyanoferrate.

7. The electrochemical cell of any one of claims 1-6, wherein the acidic electrolyte further comprises persulfate, sulfate radical, or any combination thereof.

8. The electrochemical cell of any one of claims 1-7, wherein acidic electrolyte has a pH between 1 and 4.

9. The electrochemical cell of any one of claims 1-8, wherein acidic electrolyte has a pH between about 2 and about 4.

10. The electrochemical cell of any one of claims 1-9, wherein the PFAS is selected from a perfluoroalkyl sulfonic acid, a perfluoroalkyl carboxylic acid, and a combination thereof.

11. The electrochemical cell of any one of claims 1-10, wherein the PFAS is selected from perfluorooctyl sulfonic acid, perfluorooctyl carboxylic acid, and a combination thereof.

12. The electrochemical cell of any one of claims 1-11, , wherein the Fenton activator is selected from zero valent Fe, Fe_2O_3, $FeSO_4$, FeOCl, FeOF, FeOBr, FeOI, Fe containing dual or single atom catalysts, Fe on nitrogen-doped carbon (e.g., Fe-NC or CoFe-NC), Fe containing graphitic nitride (e.g., Fe-C_3N_4), pyrolyzed Prussian blue and Prussian blue analogues, Fe on reduced graphene oxide (rGO), layered catalysts, rGO-Fe-C_3N_4, FeS_2, copper, CuO, manganese, MnO_2, cobalt, CoO, CoS_2, Co_3S_4, Co_9S_8, Fe containing metal organic frameworks, mixed metal spinels, spinel-type oxides, and any combination thereof.

13. The electrochemical cell of any one of claims 1-12, wherein the Fenton activator is a solid.

14. The electrochemical cell of any one of claims 1-13, wherein the Fenton activator is immobilized on a substrate.

15. The electrochemical cell of any one of claims 1-14, wherein the acidic electrolyte further comprises hydroxide radical.

16. The electrochemical cell of any one of claims 1-15, wherein the acidic electrolyte further comprises formate, formic acid, CO_2, F^-, HF, Cl^-, HCl, or any combination thereof.

17. The electrochemical cell of any one of claims 1-16, wherein the concentration of PFAS is between 10 and 400 ppm.

18. The electrochemical cell of any one of claims 1-17, wherein the concentration of PFAS is between 200 and 350 ppm.

19. The electrochemical cell of any one of claims 1-18, wherein the electrochemical cell is configured for batch operation.

20. The electrochemical cell of any one of claims 1-18, wherein the electrochemical cell is configured for continuous operation.

21. The electrochemical cell of any one of claims 1-20, wherein the electrochemical cell is configured for persulfate generation with less than 80% of charge passed resulting in oxygen evolution.

22. The electrochemical cell of any one of claims 1-21, wherein the electrochemical cell is configured for Faradaic efficiency greater than 20%.

23. A method for degradation of a perfluorinated or polyfluorinated alkyl substance (PFAS), the method comprising:

applying a first potential for a first application time between an anode comprising a persulfate catalyst and a redox reservoir in an electrochemical cell having an acidic electrolyte, sulfate, a Fenton activator, and a PFAS therein; and

applying a second potential for a second application time after the first application time between the redox reservoir and a cathode comprising a hydrogen peroxide catalyst in the electrochemical cell.

24. The method of claim 23, further comprising repeating application of the first potential for the first application time and the second potential for the second application time for one or more cycles.

25. The method of claim 23 or 24, further comprising introducing a contaminated feedstock comprising the PFAS into the electrochemical cell.

26. The method of claim 25, further comprising concentrating the contaminated feedstock prior to introduction into the electrochemical cell.

27. The method of any one of claims 25-26, wherein the contaminated feedstock has a PFAS concentration between 10 and 400 ppm.

28. The method of any one of claims 23-27, further comprising recovering fluoride (F^-).

29. The method of claim 28, wherein the fluoride (F^-) is recovered as FeOF.

30. The method of any one of claims 23-29, wherein the first potential, the second potential, or both the first potential and the second potential is between -0.2 and 0.7 V vs SCE.

31. The method of any one of claims 23-23, wherein the electrochemical cell is the electrochemical cell according to any one of claims 1-22.

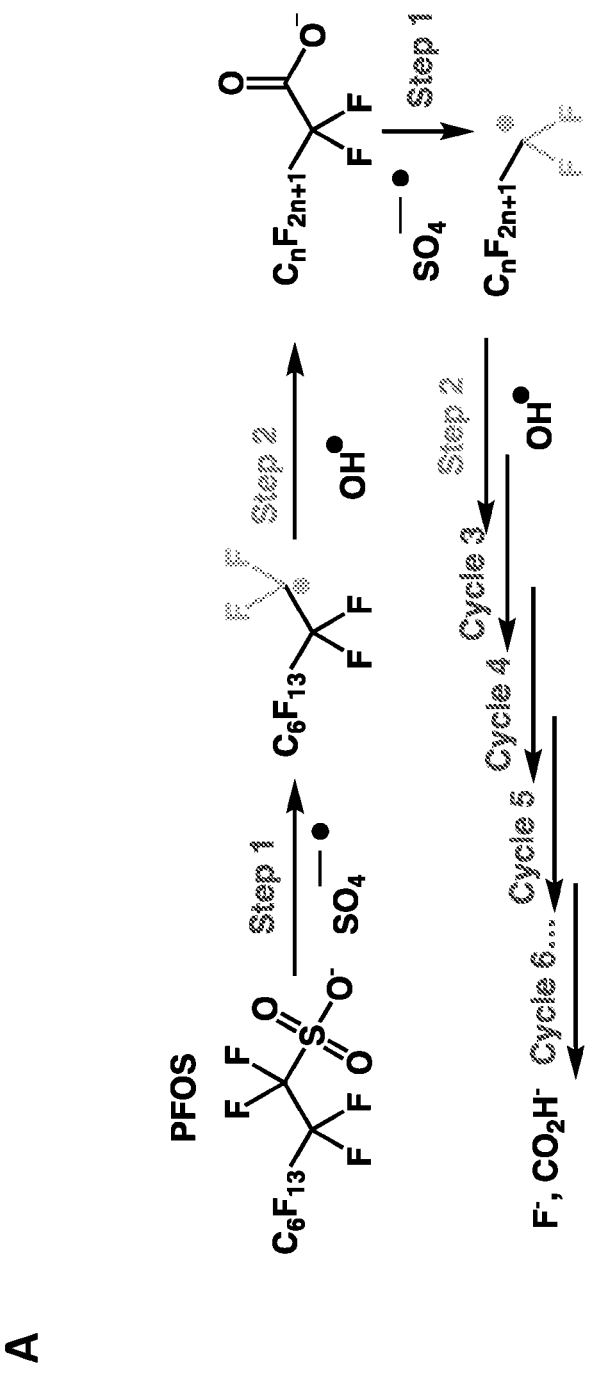
A
PFOS
Step 1
Step 2
Step 1
Step 2
Cycle 3
Cycle 4
Cycle 5
Cycle 6...
F⁻, CO2H⁻

FIG. 1

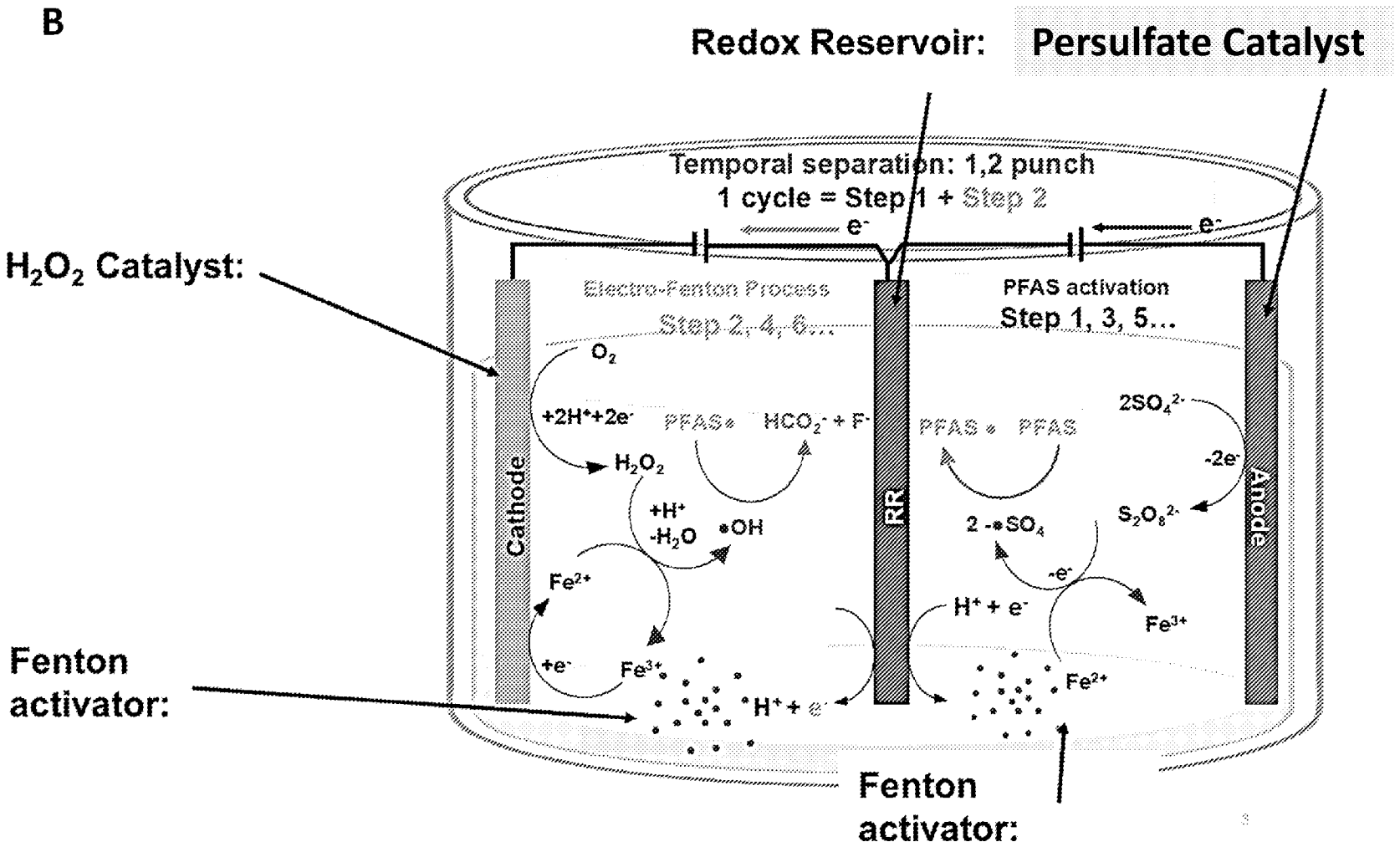
B
Redox Reservoir:
Persulfate Catalyst
Temporal separation: 1,2 punch
1 cycle = Step 1 + Step 2
H_2O_2 Catalyst:
Electro-Fenton Process
Step 2, 4, 6...
PFAS activation
Step 1, 3, 5...
Cathode
RR
Anode
O_2
$+2H^+ + 2e^-$
PFAS
$HCO_2^- + F^-$
H_2O_2
$+H^+$
$-H_2O$
$^\bullet OH$
Fe^{2+}
$+e^-$
Fe^{3+}
$H^+ + e^-$
$2SO_4^{2-}$
$-2e^-$
$S_2O_8^{2-}$
$2\ ^\bullet SO_4^-$
$-e^-$
Fe^{3+}
Fe^{2+}
Fenton activator:
Fenton activator:

FIG. 1 cont'd

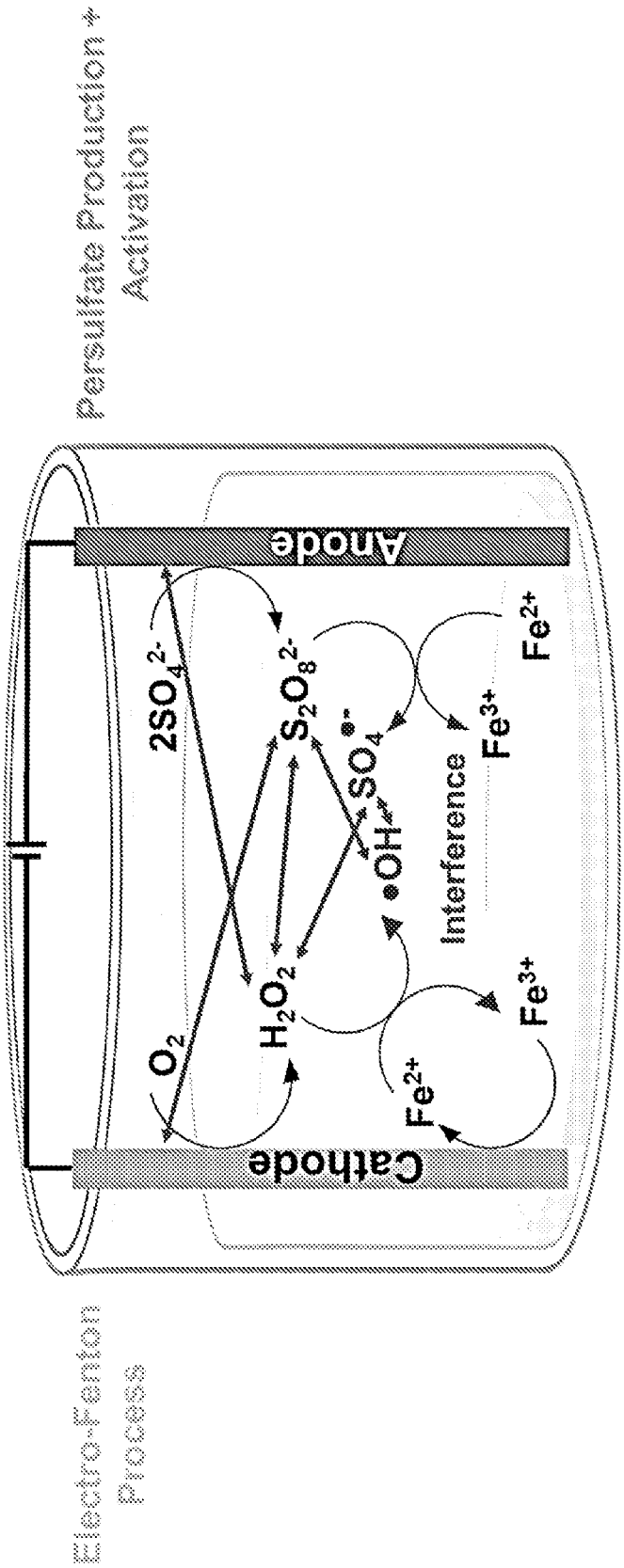
C
Persulfate Production +
Activation
Anode
Cathode
$2SO_4^{2-}$
$S_2O_8^{2-}$
$SO_4^{\bullet-}$
$\bullet OH$
H_2O_2
O_2
Fe^{2+}
Fe^{3+}
Interference
Electro-Fenton
Process

FIG. 1 cont'd

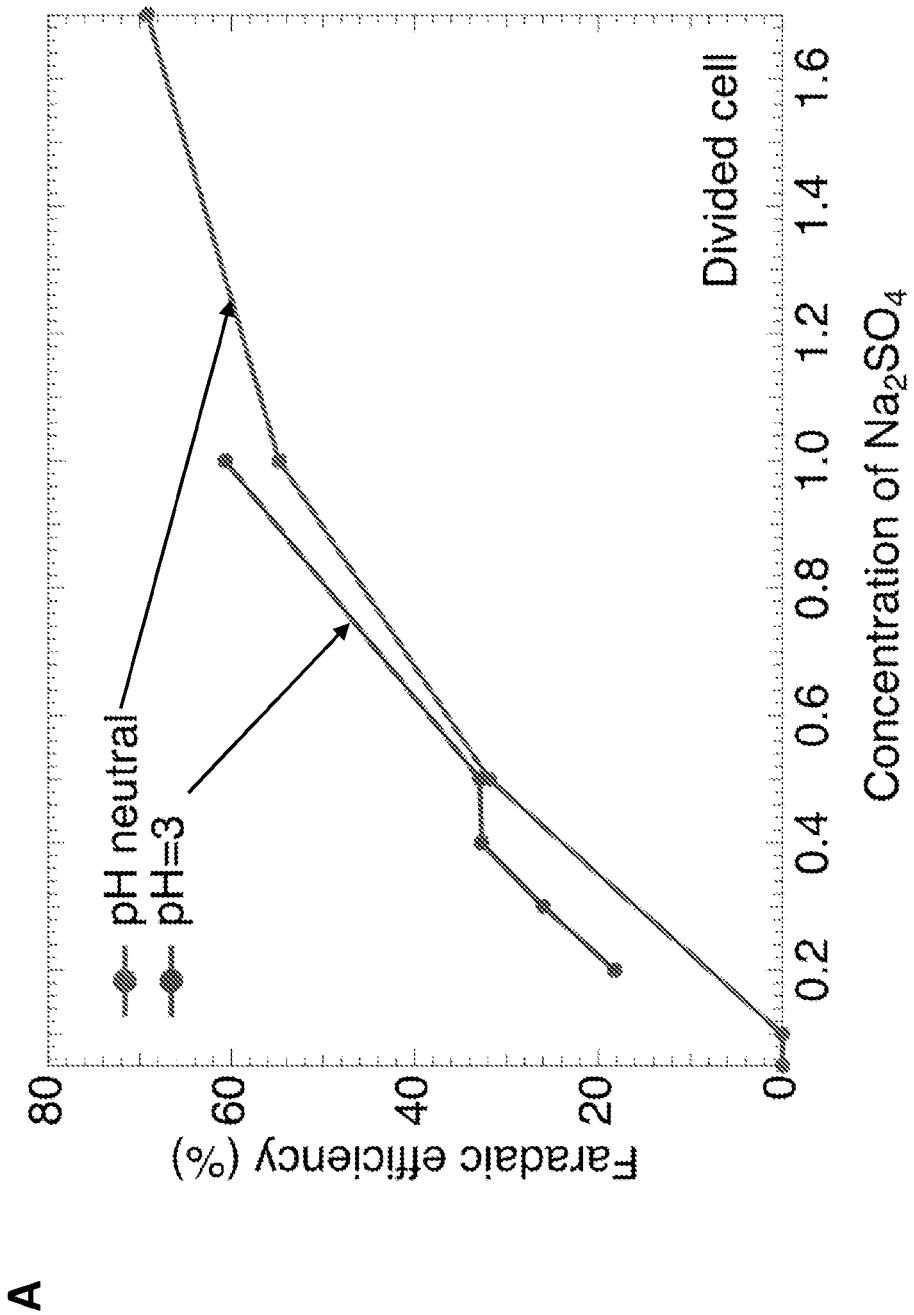
A
Faradaic efficiency (%)
0
20
40
60
80
0.2
0.4
0.6
0.8
1.0
1.2
1.4
1.6
Concentration of Na_2SO_4
Divided cell
pH neutral
pH=3

FIG. 2

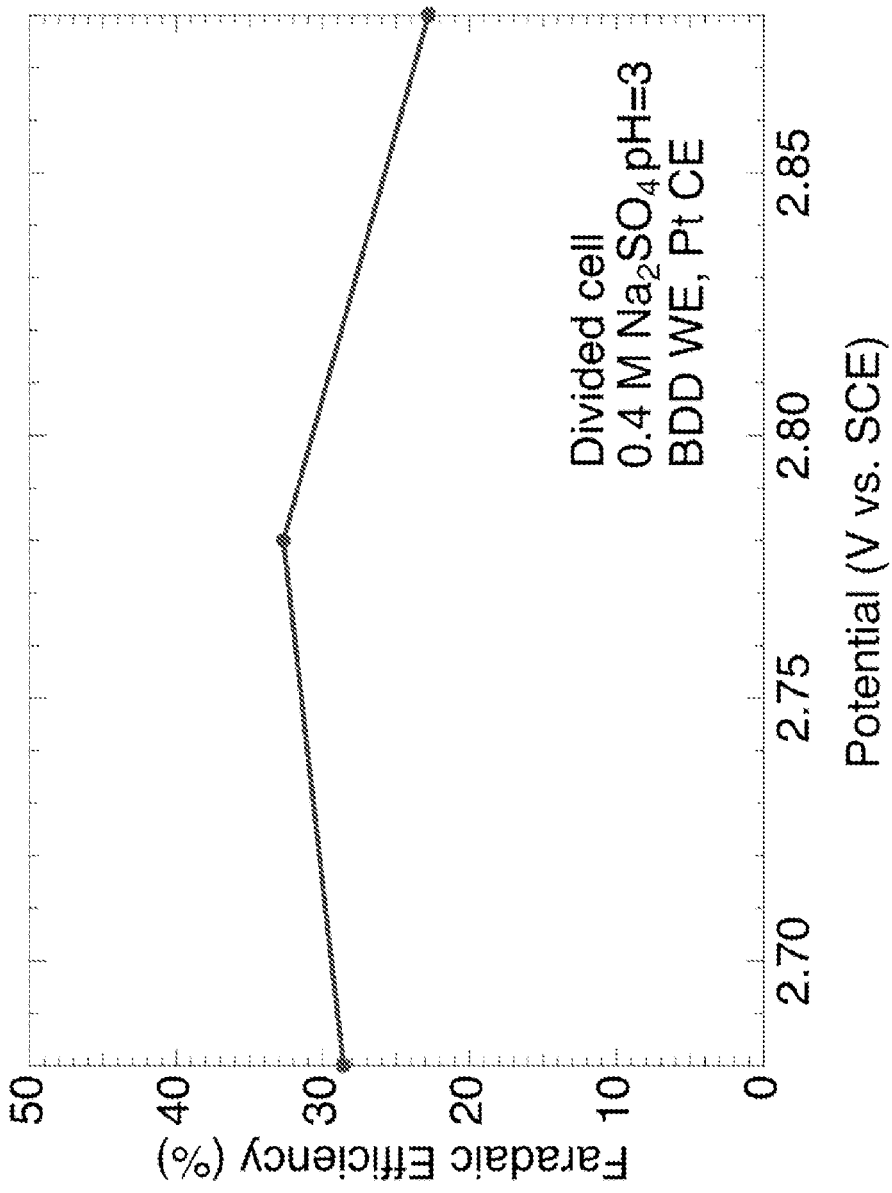
B
Faradaic Efficiency (%)
50
40
30
20
10
0
2.70
2.75
2.80
2.85
Potential (V vs. SCE)
Divided cell
0.4 M Na_2SO_4 pH=3
BDD WE, Pt CE

FIG. 2 cont'd

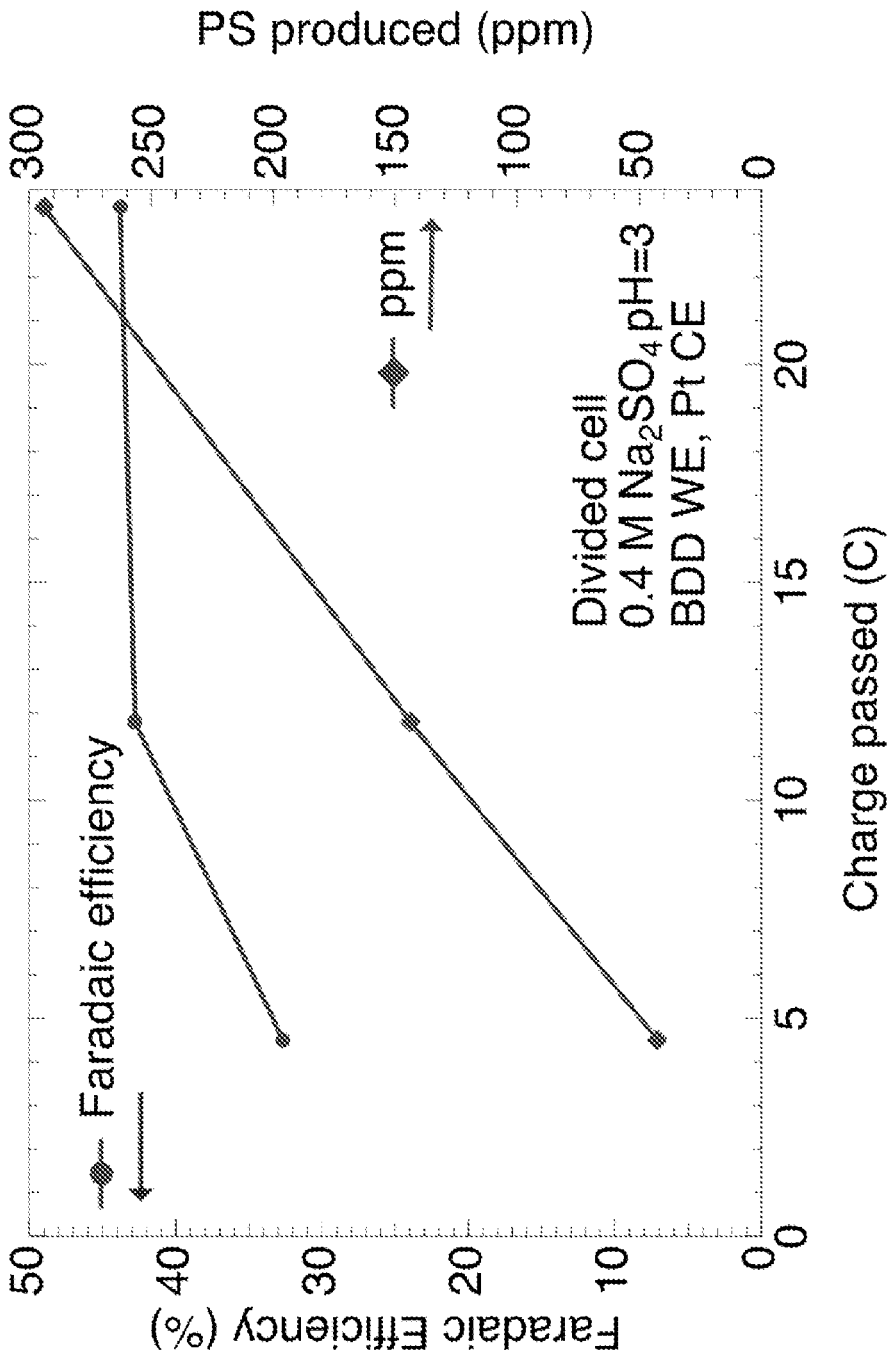
PS produced (ppm)
300
250
200
150
100
50
0
ppm
Faradaic efficiency
Divided cell
0.4 M Na_2SO_4 pH=3
BDD WE, Pt CE
50
40
30
20
10
0
Faradaic Efficiency (%)
0
5
10
15
20
Charge passed (C)

C

FIG. 2 cont'd

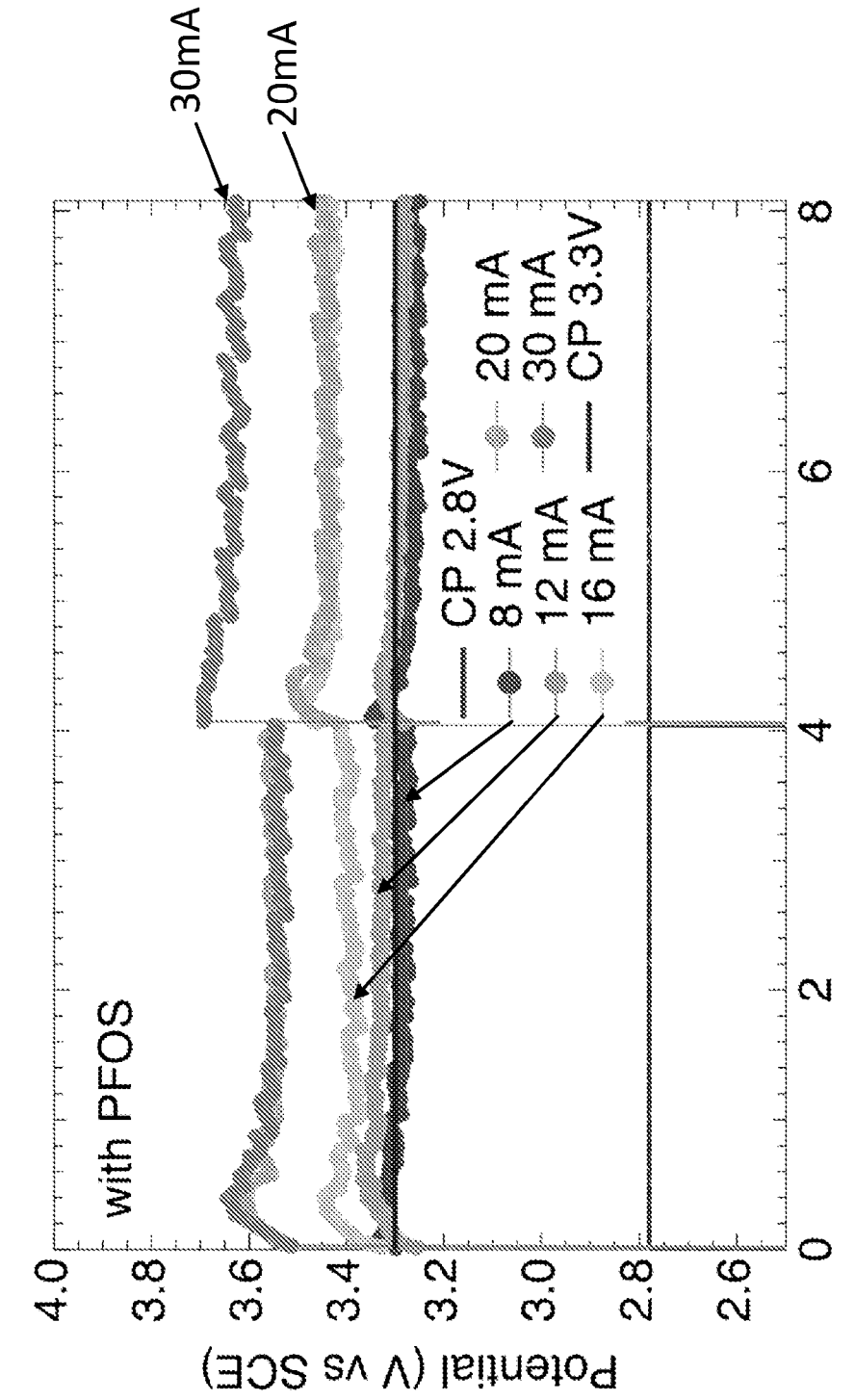
D
Potential (V vs SCE)
4.0
3.8
3.6
3.4
3.2
3.0
2.8
2.6
0
2
4
6
8
Charge passed (C)
with PFOS
30mA
20mA
CP 2.8V
8 mA
12 mA
16 mA
20 mA
30 mA
CP 3.3V

FIG. 2 cont'd

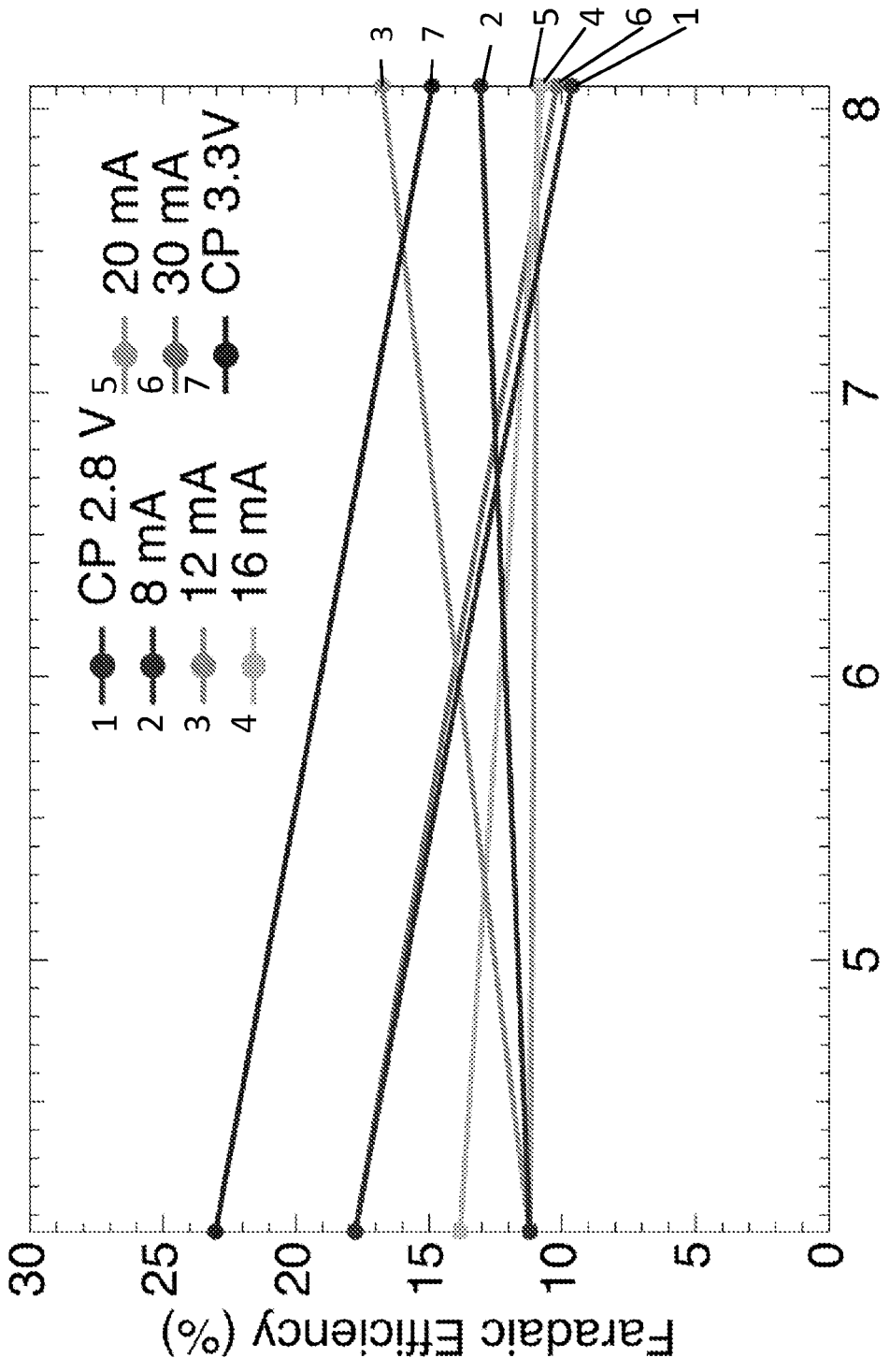
Faradaic Efficiency (%)
0
5
10
15
20
25
30
5
6
7
8
Charge (C)
1 CP 2.8 V
2 8 mA
3 12 mA
4 16 mA
5 20 mA
6 30 mA
7 CP 3.3V
3
7
2
5
4
6
1

FIG. 2 cont'd

E

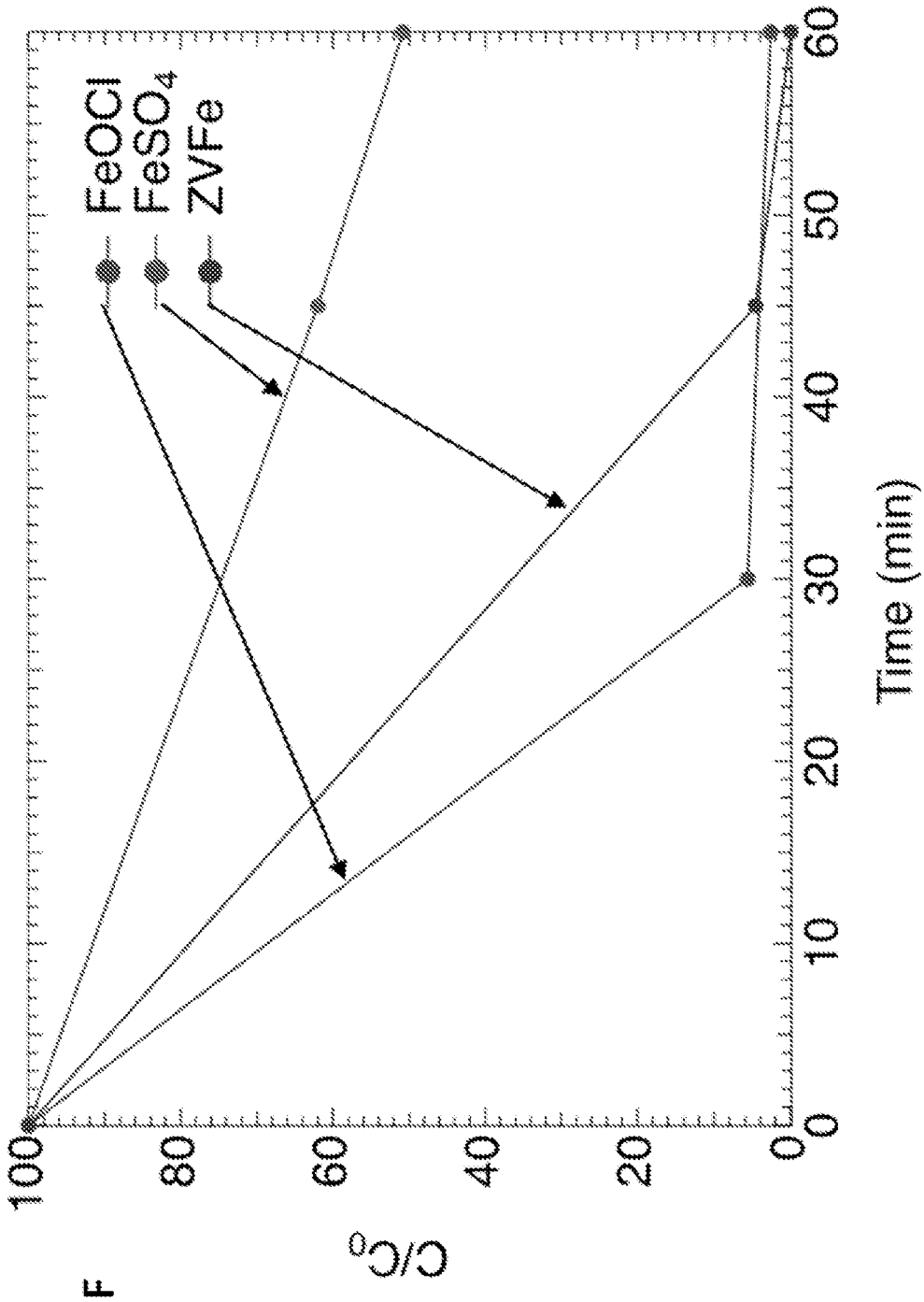

FIG. 2 cont'd

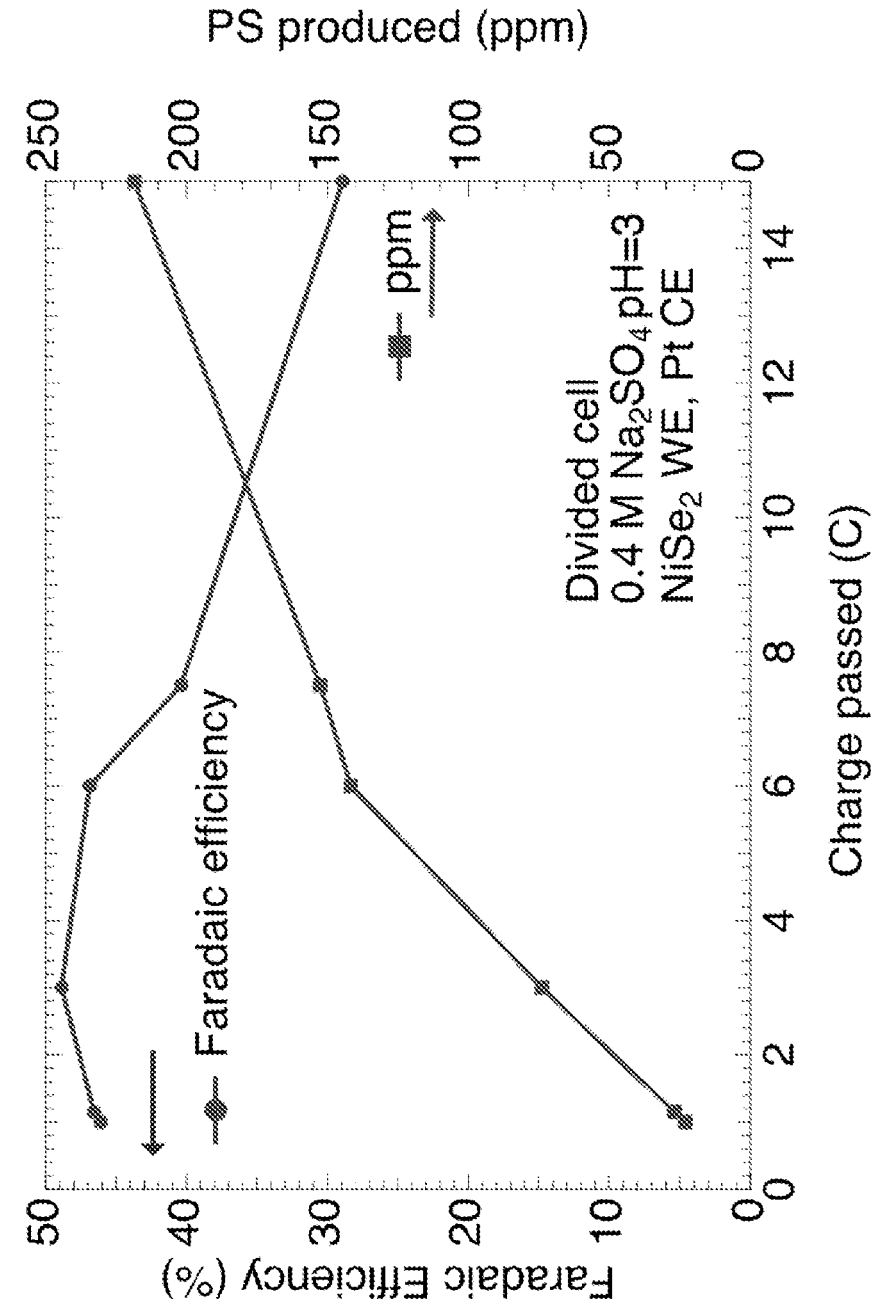
PS produced (ppm)
250
200
150
100
50
0
ppm
Divided cell
0.4 M Na_2SO_4 pH=3
$NiSe_2$ WE, Pt CE
Faradaic efficiency
50
40
30
20
10
0
Faradaic Efficiency (%)
0
2
4
6
8
10
12
14
Charge passed (C)

G

FIG. 2

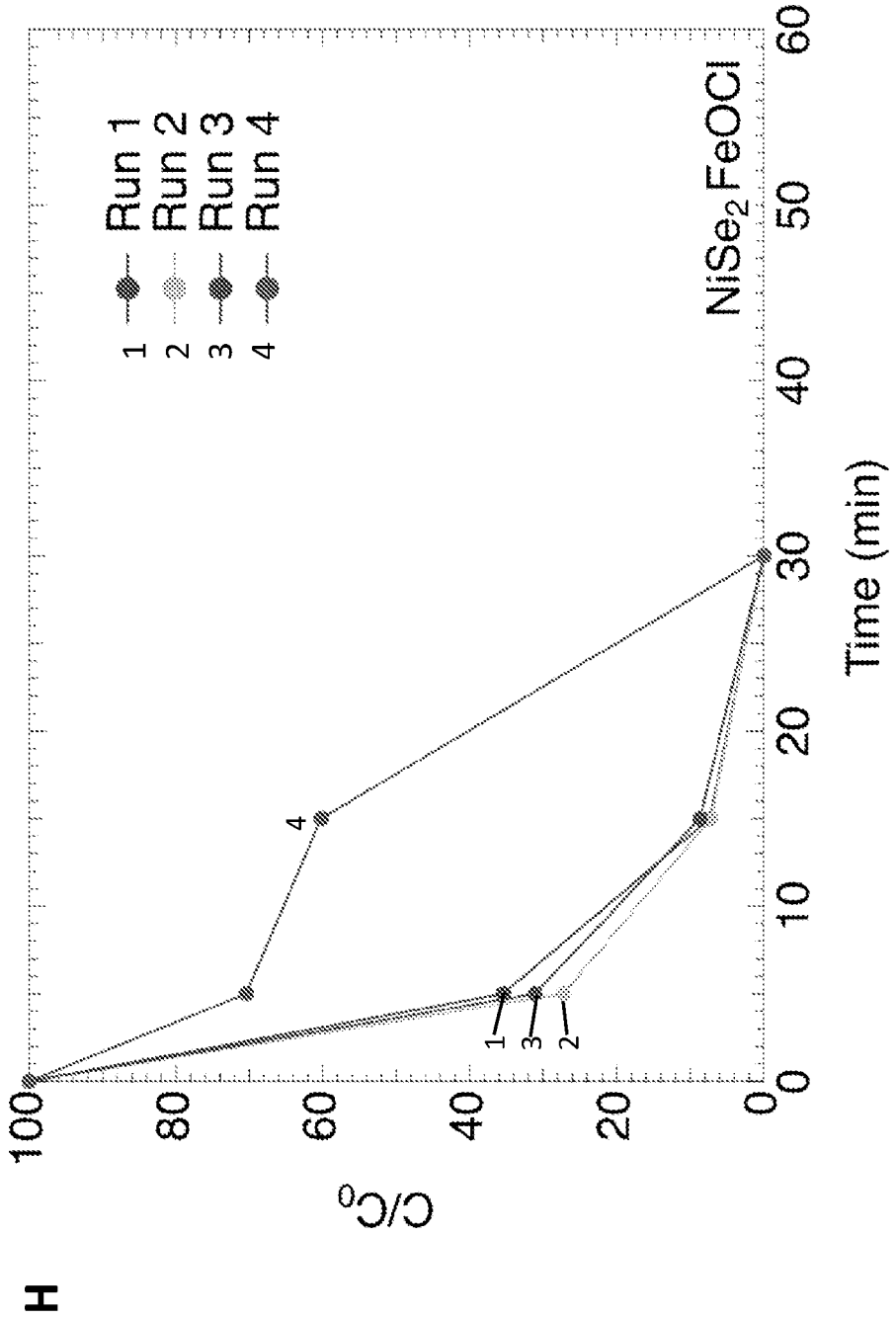
H
C/C0
Time (min)
NiSe2 FeOCl
Run 1
Run 2
Run 3
Run 4
1
2
3
4
0
20
40
60
80
100
0
10
20
30
40
50
60

FIG. 2 cont'd

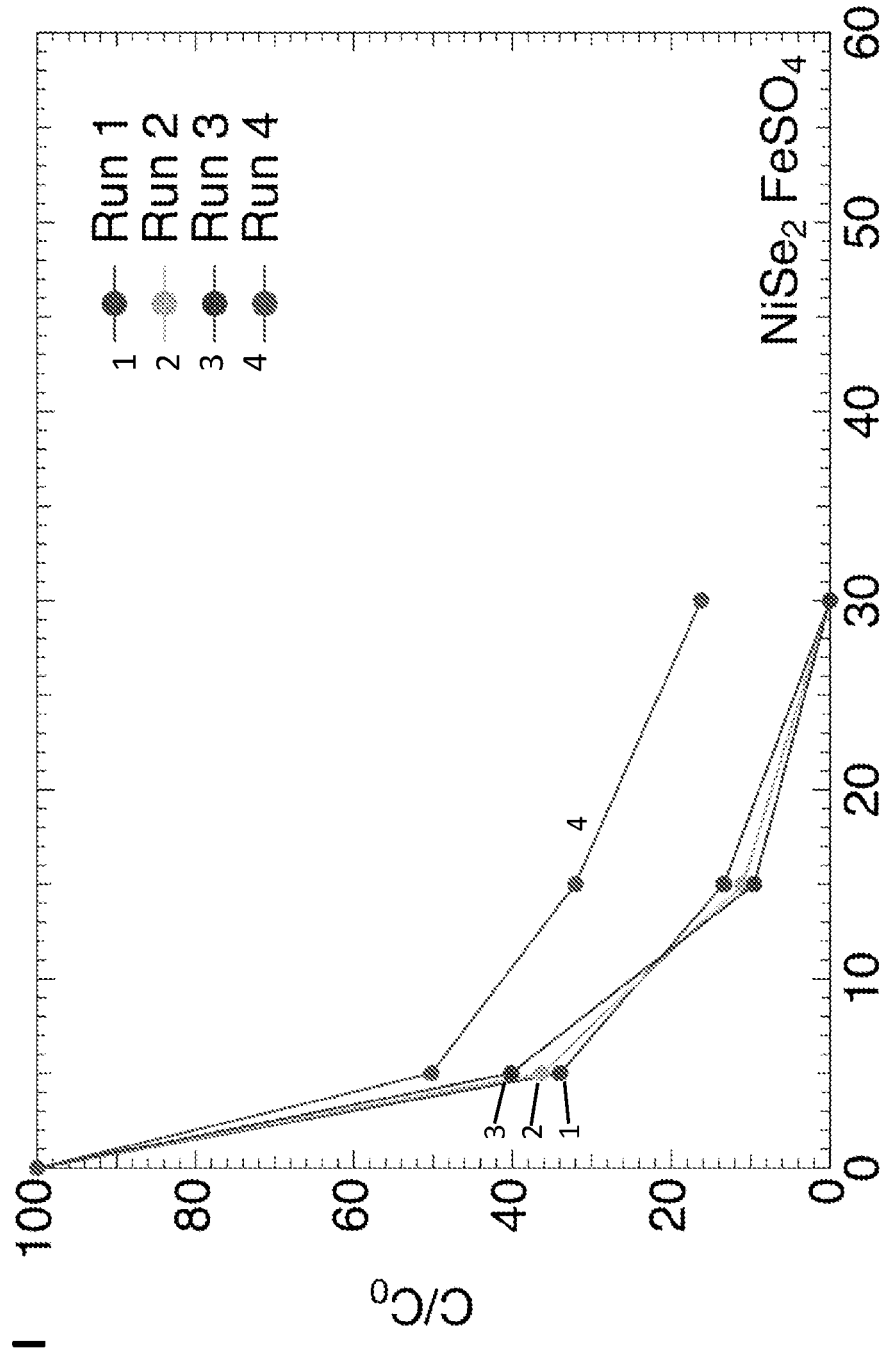
Run 1
Run 2
Run 3
Run 4
1
2
3
4
NiSe2 FeSO4
C/C0
Time (min)
0
10
20
30
40
50
60
20
40
60
80
100

FIG. 2 cont'd

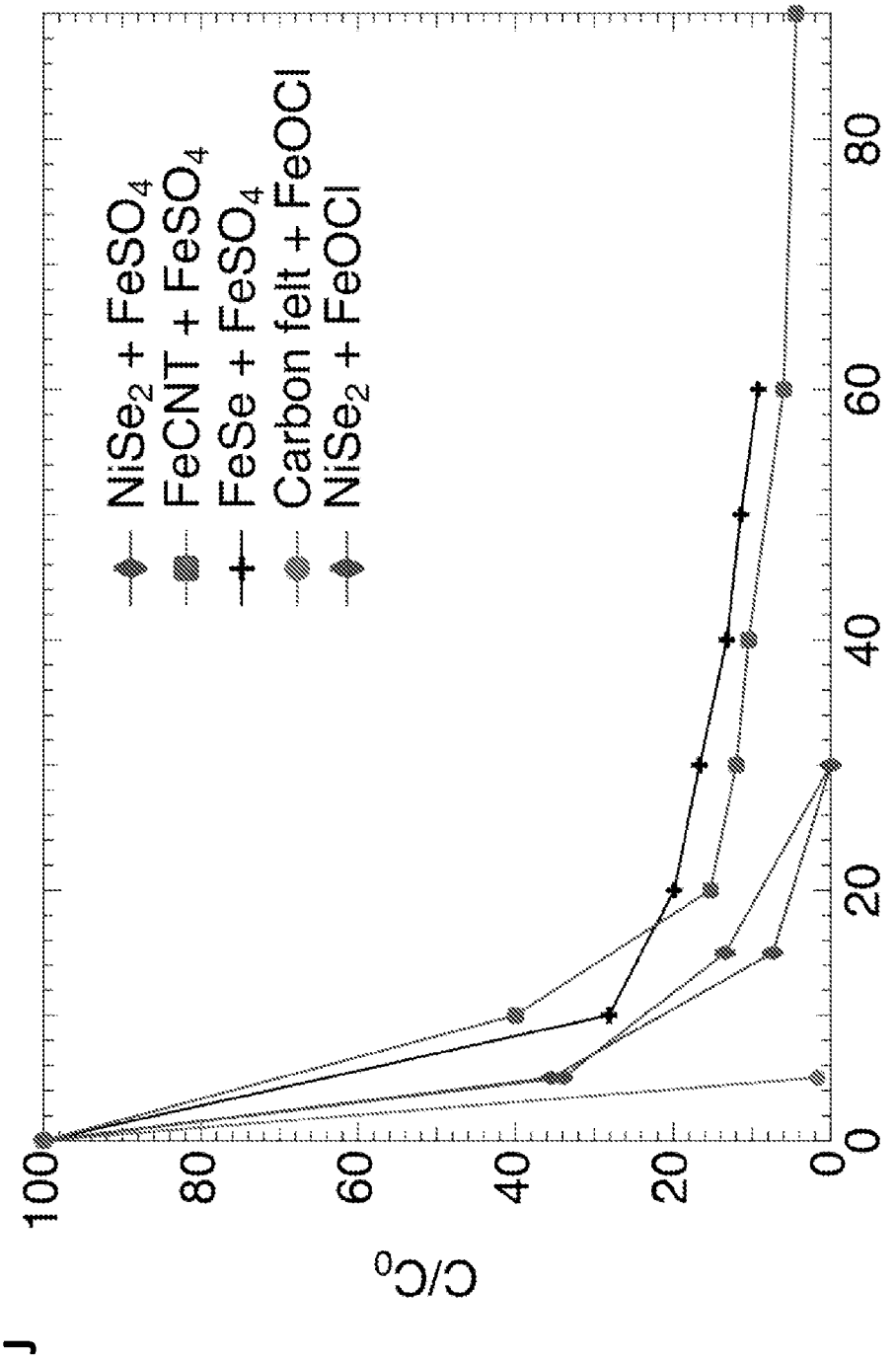
J
C/C0
100
80
60
40
20
0
0
20
40
60
80
Time (min)
NiSe2 + FeSO4
FeCNT + FeSO4
FeSe + FeSO4
Carbon felt + FeOCl
NiSe2 + FeOCl

FIG. 2- cont'd

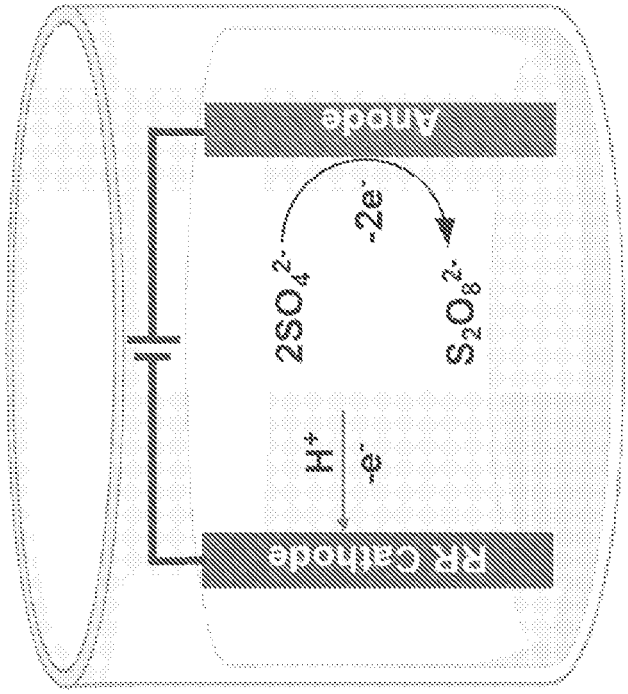
Anode
$2SO_4^{2-}$
-2e⁻
$S_2O_8^{2-}$
H^+
-e⁻
RR Cathode

B

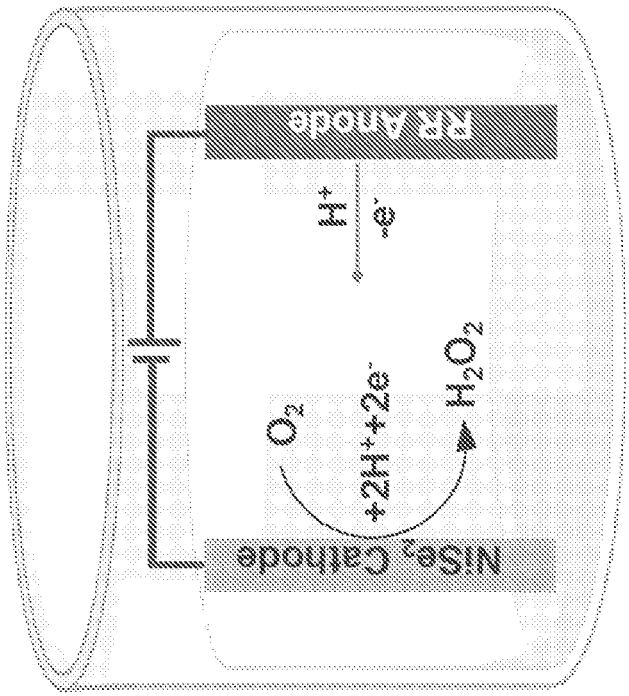
RR Anode
H^+
-e⁻
O_2
$+2H^+ + 2e^-$
H_2O_2
$NiSe_2$ Cathode

A

FIG. 3

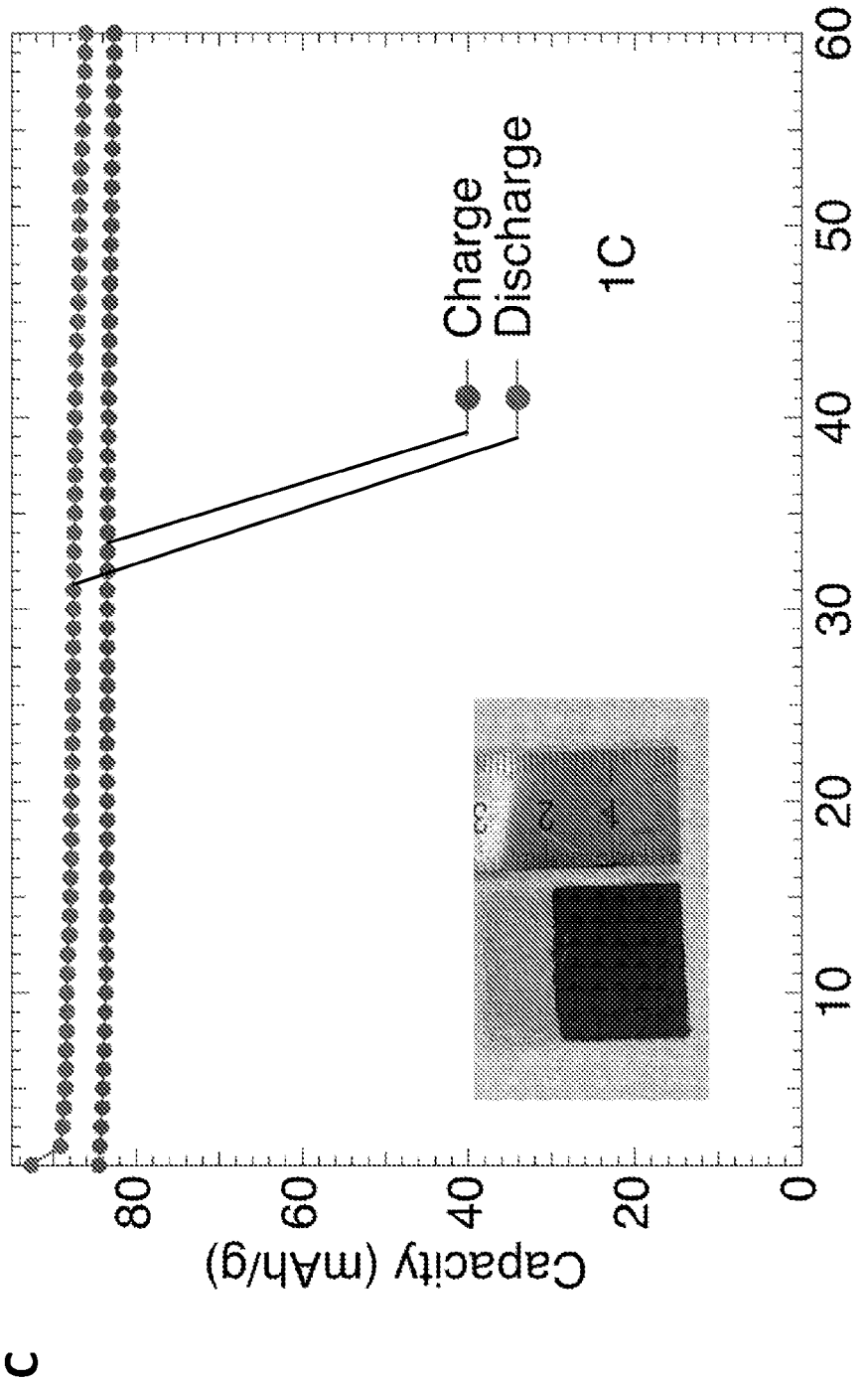
C
Capacity (mAh/g)
0
20
40
60
80
10
20
30
40
50
60
Cycle number
Charge
Discharge
1C

FIG. 3 cont'd

D

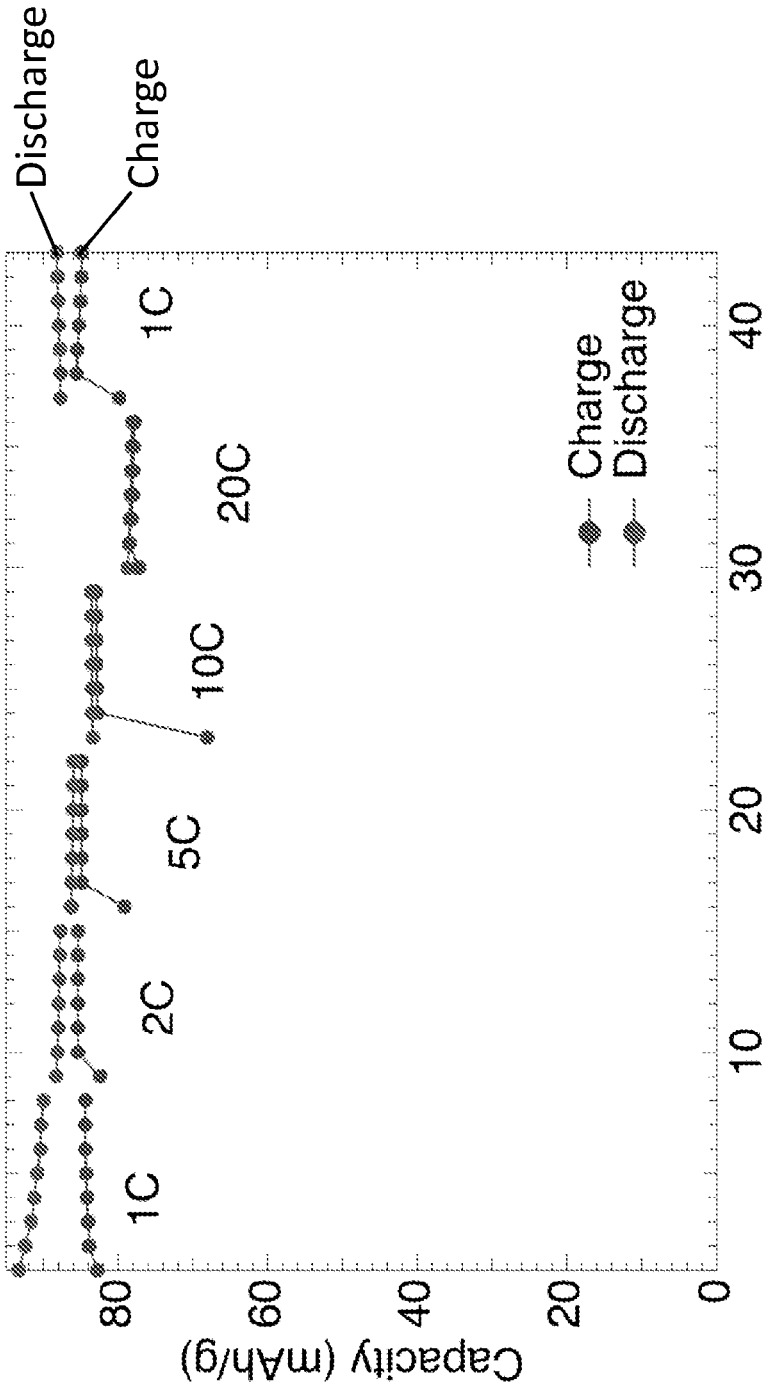
Discharge
Charge
1C
2C
5C
10C
20C
1C
Charge
Discharge
Capacity (mAh/g)
0
20
40
60
80
10
20
30
40
Cycle number

FIG. 3 cont'd

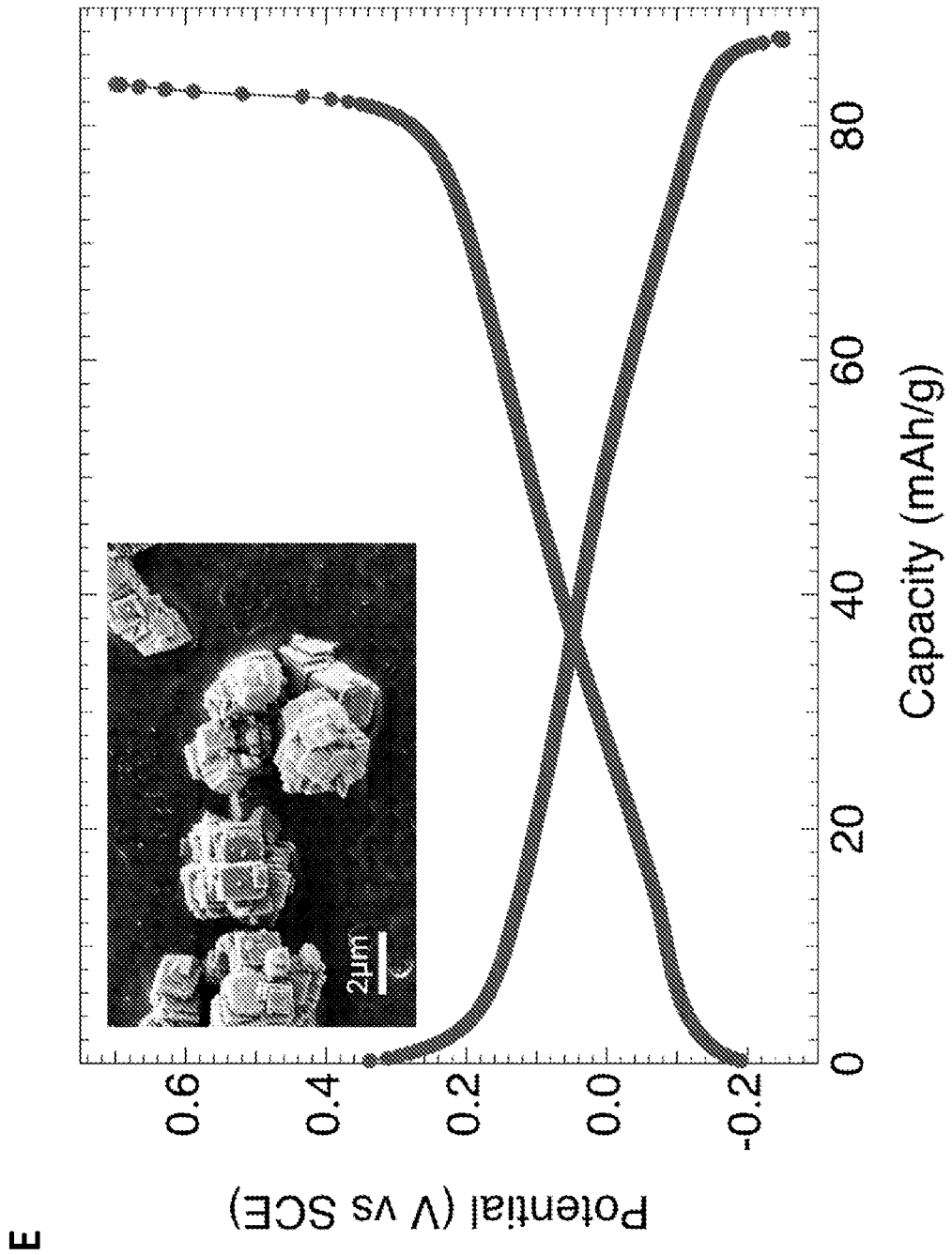
E
Potential (V vs SCE)
0.6
0.4
0.2
0.0
-0.2
0
20
40
60
80
Capacity (mAh/g)
2μm

FIG. 3 cont'd

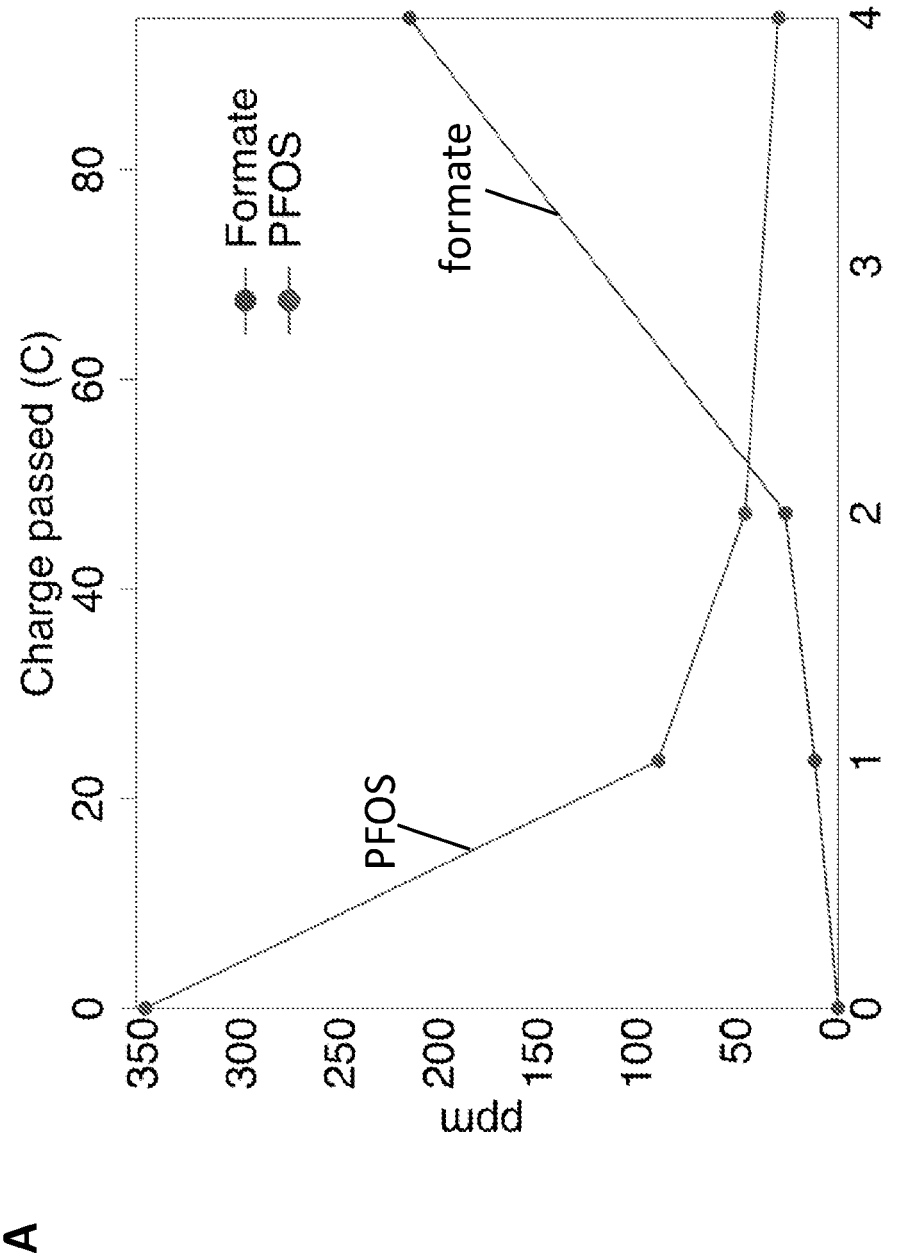
A
ppm
350
300
250
200
150
100
50
0
Charge passed (C)
0
20
40
60
80
Cycle
0
1
2
3
4
Formate
PFOS
formate
PFOS

FIG. 4

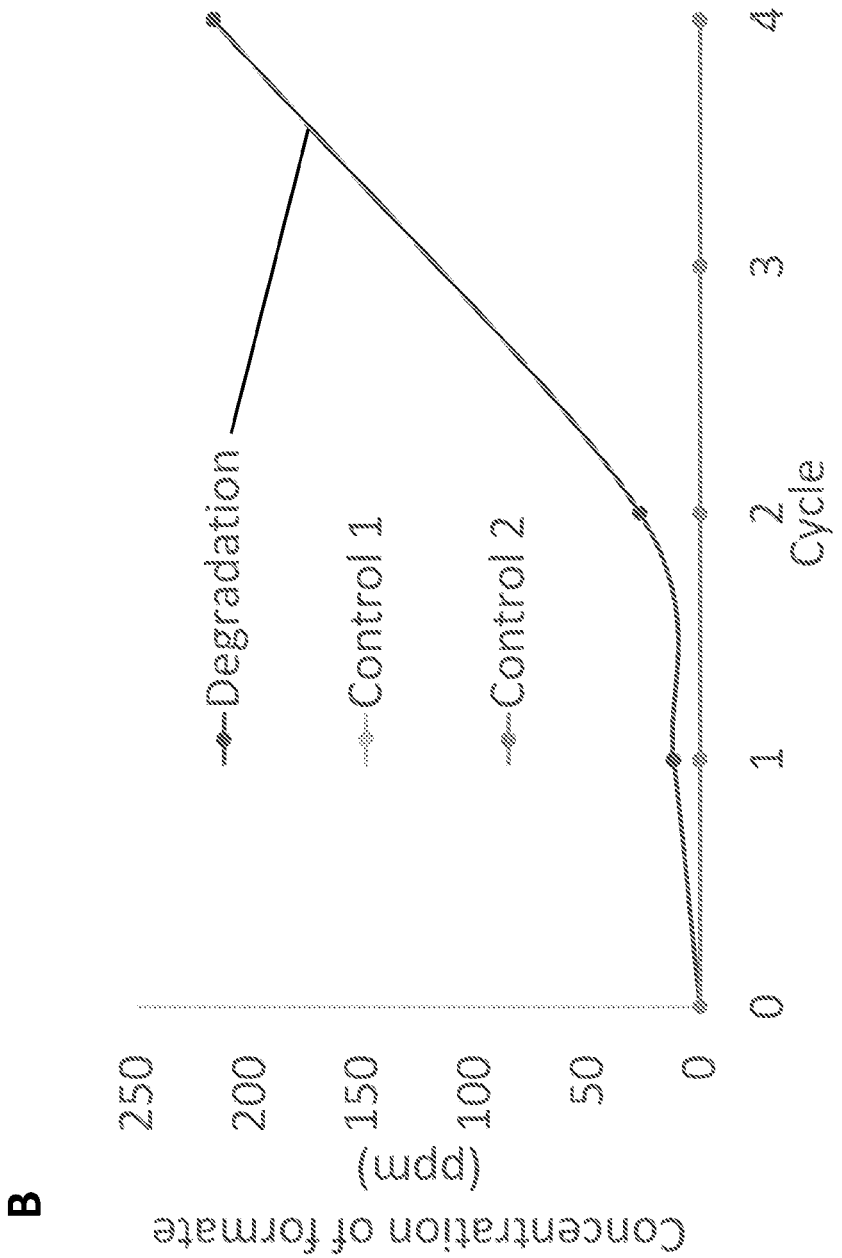
B
Concentration of formate
(ppm)
250
200
150
100
50
0
0
1
2
3
4
Cycle
Degradation
Control 1
Control 2

FIG. 4 cont'd

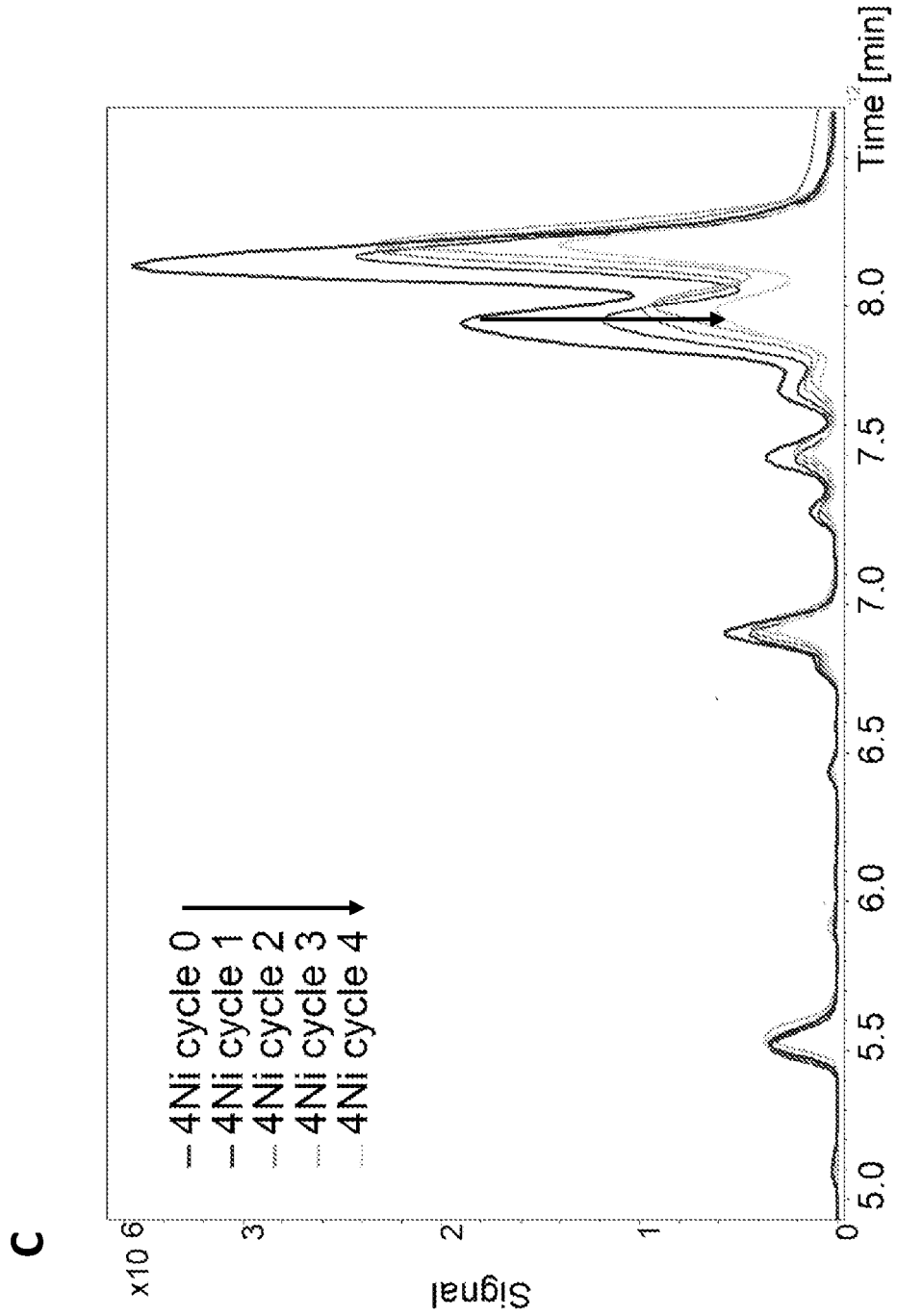
C
x10 6
3
2
1
0
Signal
5.0
5.5
6.0
6.5
7.0
7.5
8.0
Time [min]
4Ni cycle 0
4Ni cycle 1
4Ni cycle 2
4Ni cycle 3
4Ni cycle 4

FIG. 4 cont'd

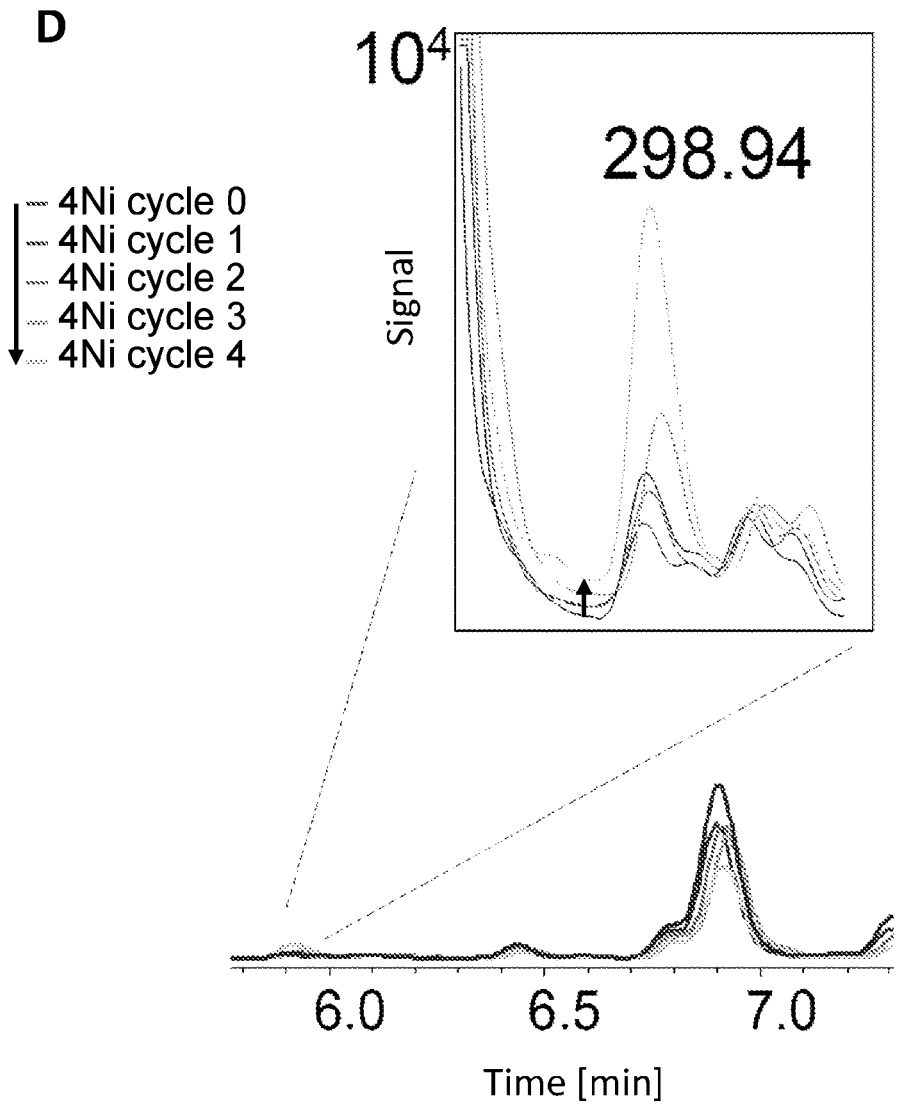
D
4Ni cycle 0
4Ni cycle 1
4Ni cycle 2
4Ni cycle 3
4Ni cycle 4
10^4
298.94
Signal
6.0
6.5
7.0
Time [min]

FIG. 4 cont'd

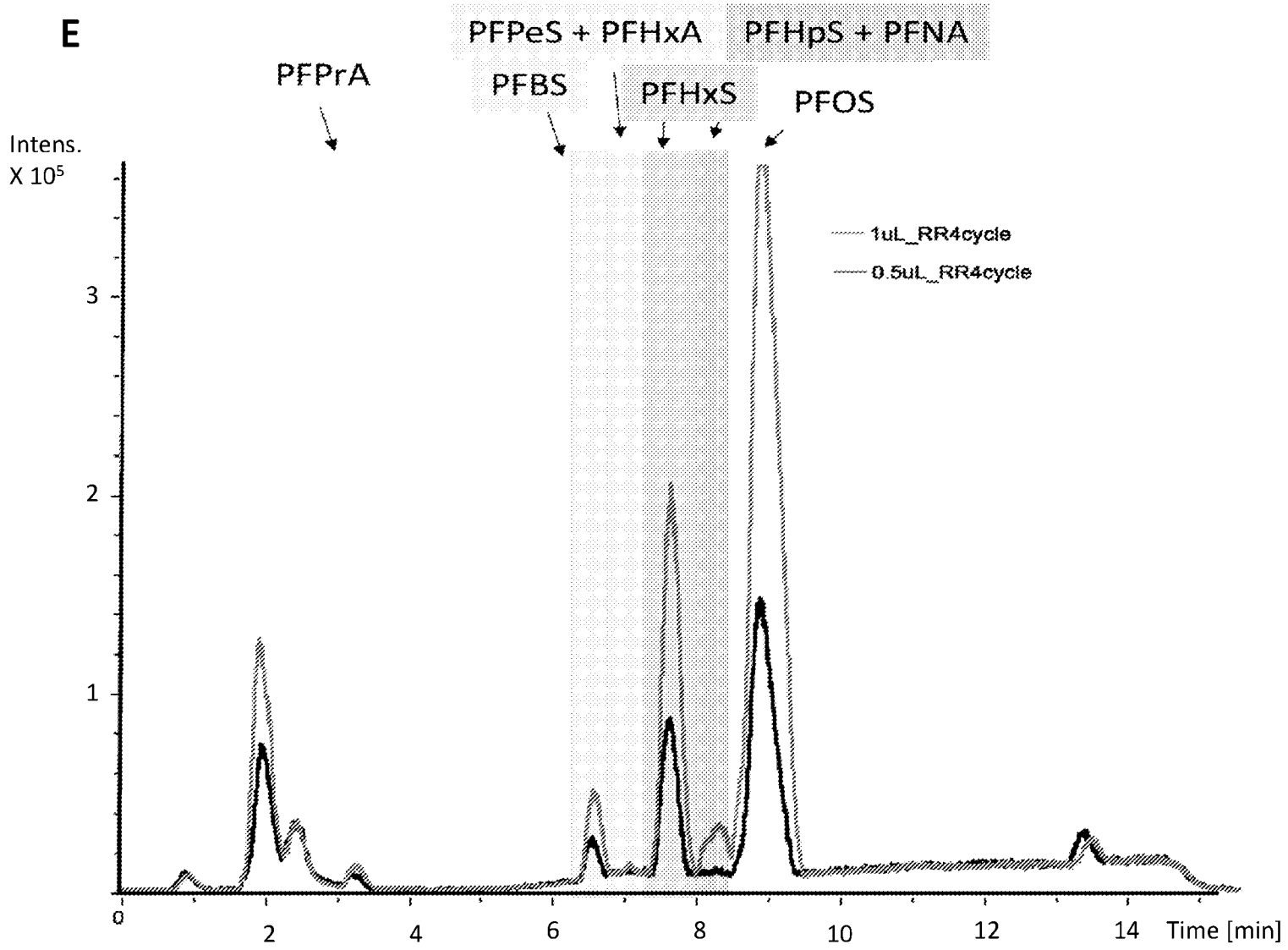
E
PFPeS + PFHxA
PFHpS + PFNA
PFPrA
PFBS
PFHxS
PFOS
Intens.
X 10^5
1uL_RR4cycle
0.5uL_RR4cycle
3
2
1
0
2
4
6
8
10
12
14
Time [min]

FIG. 4 cont'd

FIG. 4 cont'd

F

sulfate

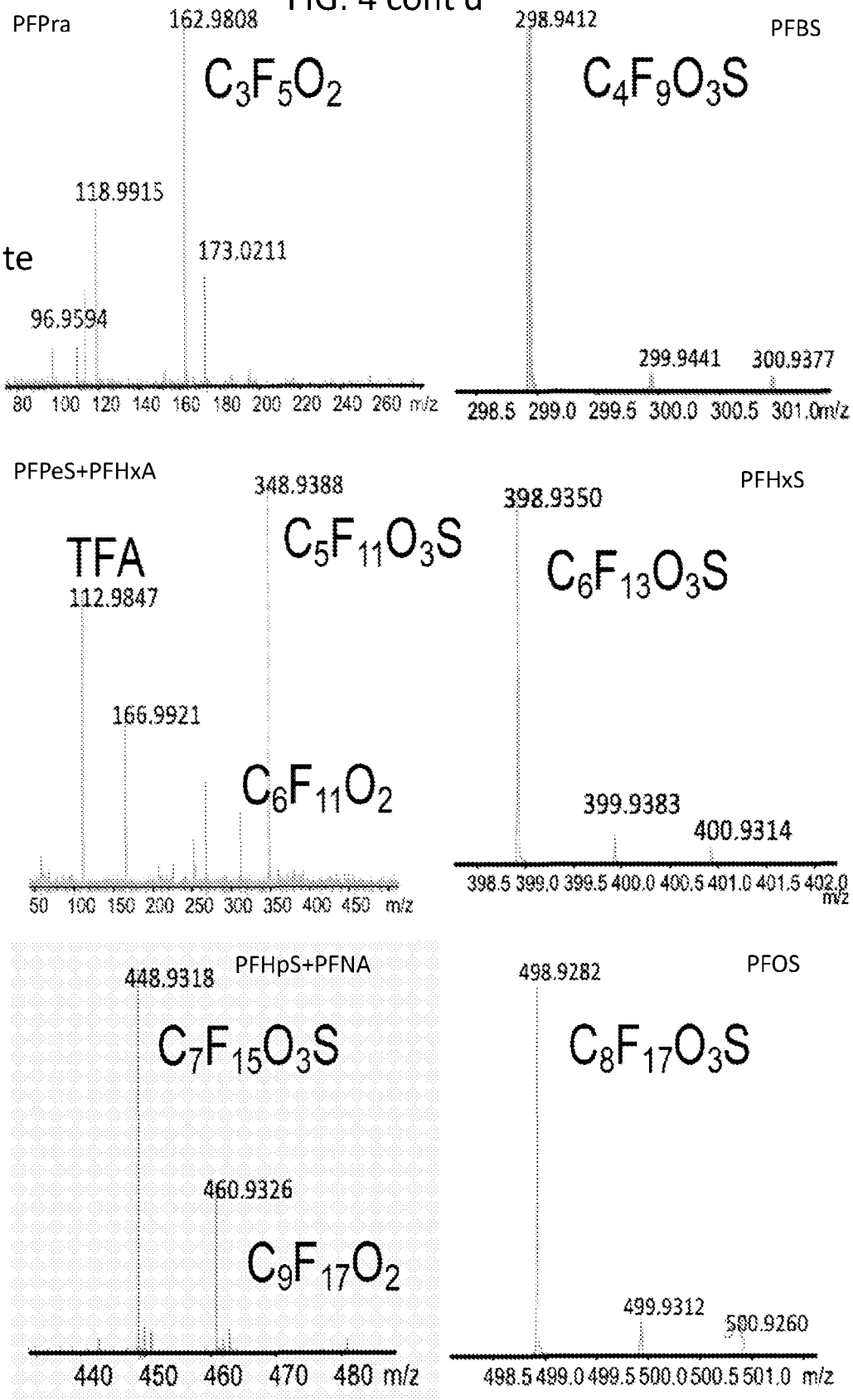

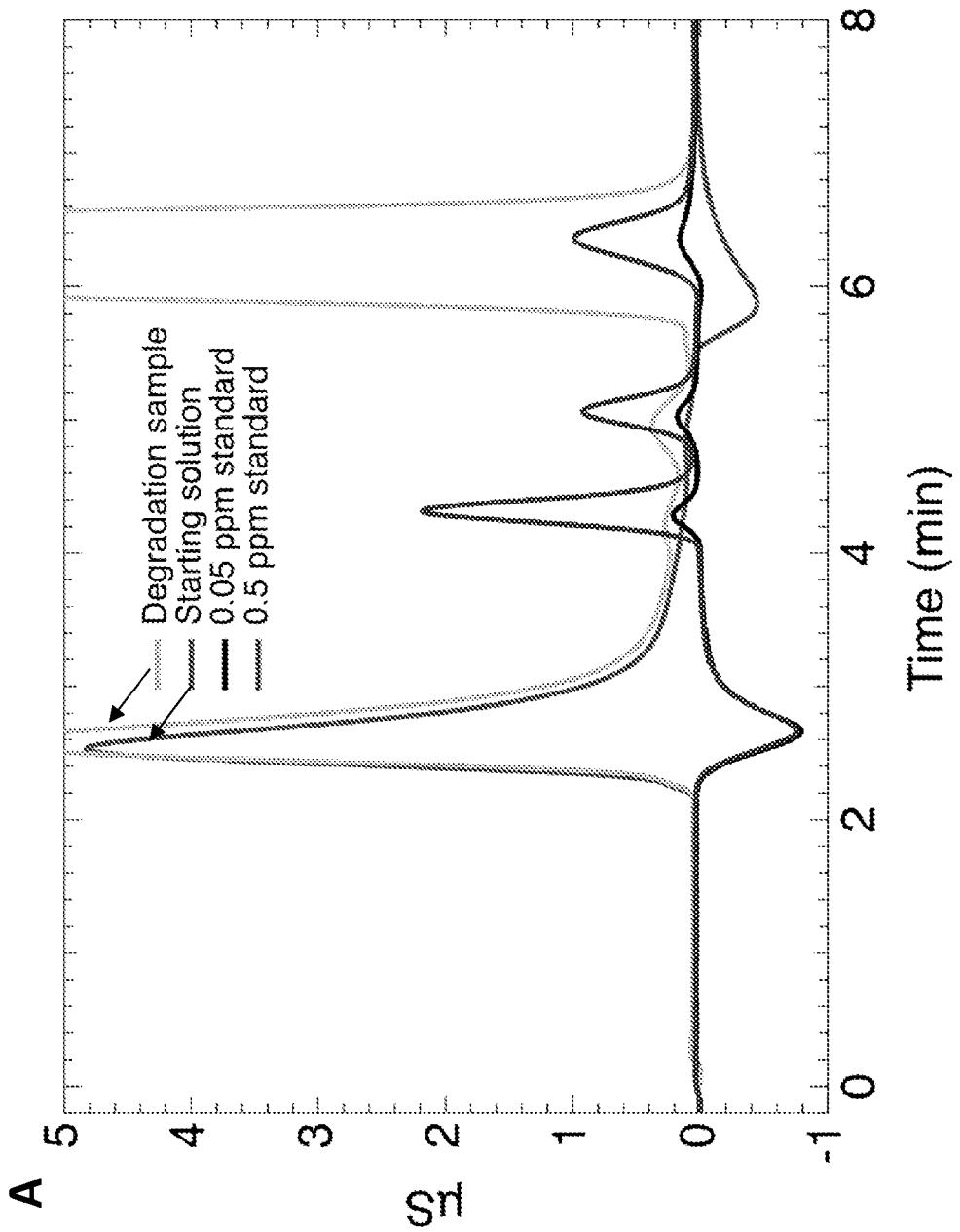
A
μS
5
4
3
2
1
0
-1
0
2
4
6
8
Time (min)
Degradation sample
Starting solution
0.05 ppm standard
0.5 ppm standard

FIG. 5

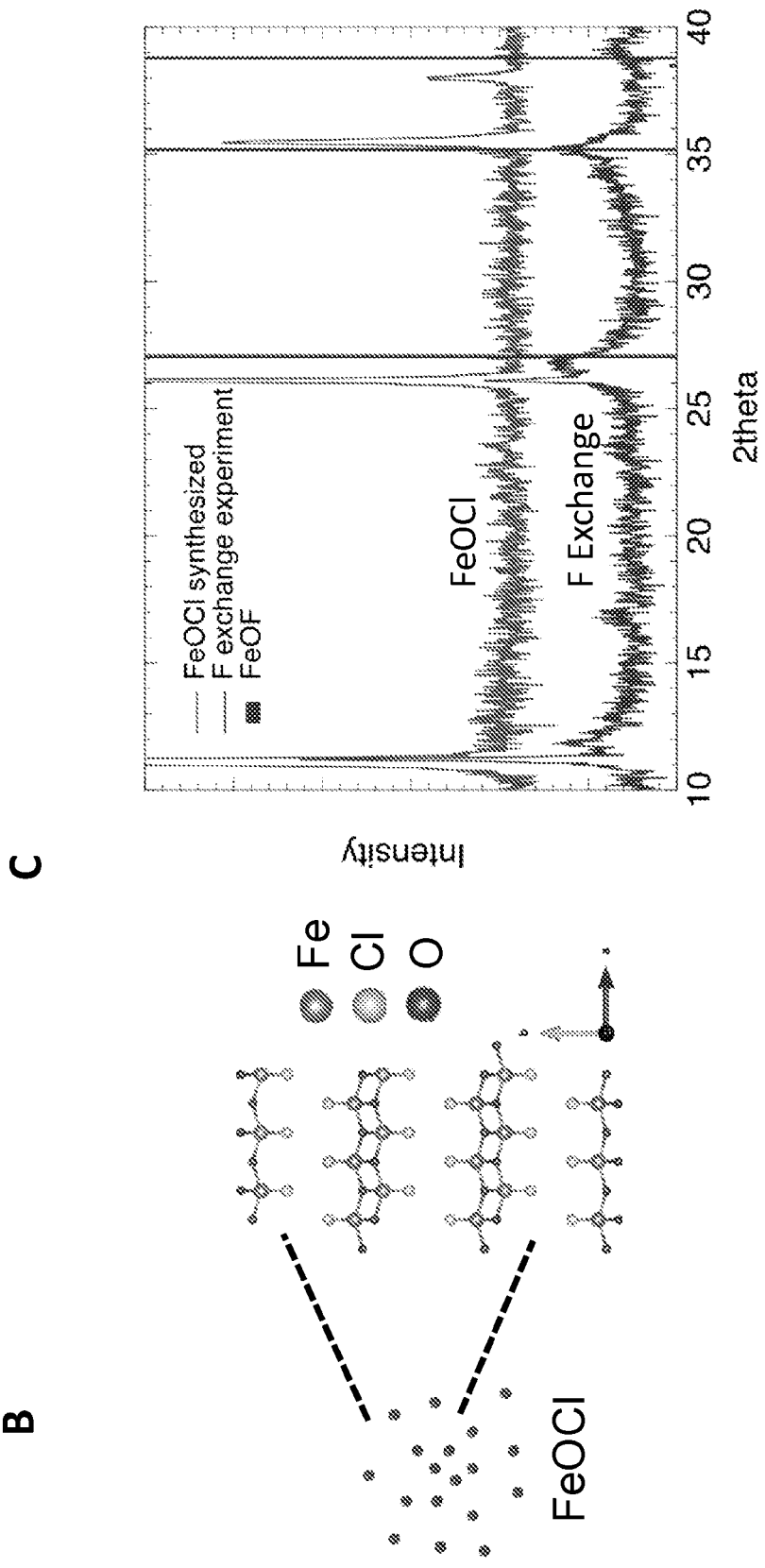
B
Fe
Cl
O
FeOCl
C
Intensity
FeOCl synthesized
F exchange experiment
FeOF
FeOCl
F Exchange
10
15
20
25
30
35
40
2theta

FIG. 5 cont'd

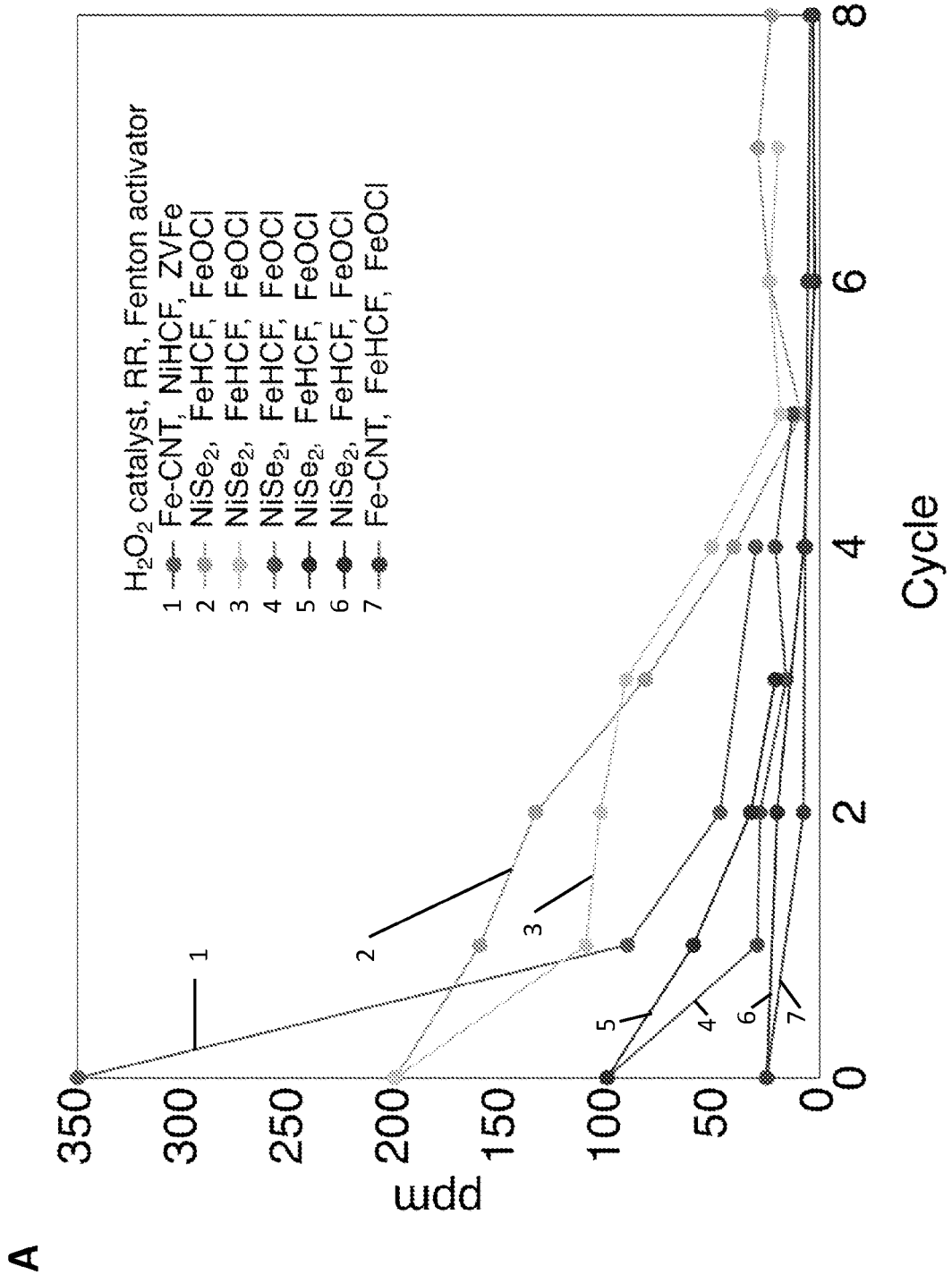
A
ppm
Cycle
0
50
100
150
200
250
300
350
0
2
4
6
8
H_2O_2 catalyst, RR, Fenton activator
1 Fe-CNT, NiHCF, ZVFe
2 $NiSe_2$, FeHCF, FeOCl
3 $NiSe_2$, FeHCF, FeOCl
4 $NiSe_2$, FeHCF, FeOCl
5 $NiSe_2$, FeHCF, FeOCl
6 $NiSe_2$, FeHCF, FeOCl
7 Fe-CNT, FeHCF, FeOCl

FIG. 6

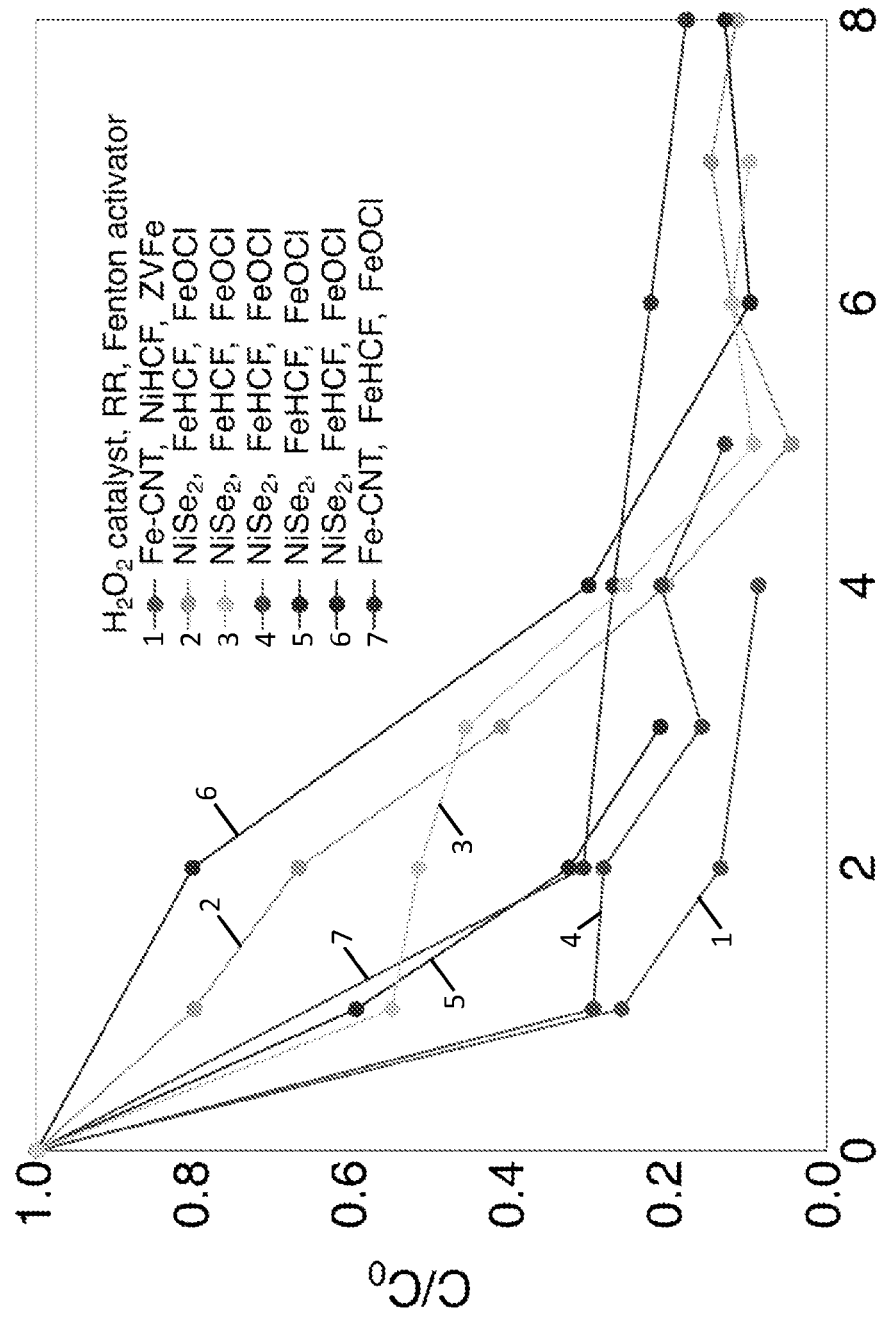
B
C/C0
Cycle
H2O2 catalyst, RR, Fenton activator
1 Fe-CNT, NiHCF, ZVFe
2 NiSe2, FeHCF, FeOCl
3 NiSe2, FeHCF, FeOCl
4 NiSe2, FeHCF, FeOCl
5 NiSe2, FeHCF, FeOCl
6 NiSe2, FeHCF, FeOCl
7 Fe-CNT, FeHCF, FeOCl
0.0
0.2
0.4
0.6
0.8
1.0
0
2
4
6
8

FIG. 6 cont'd

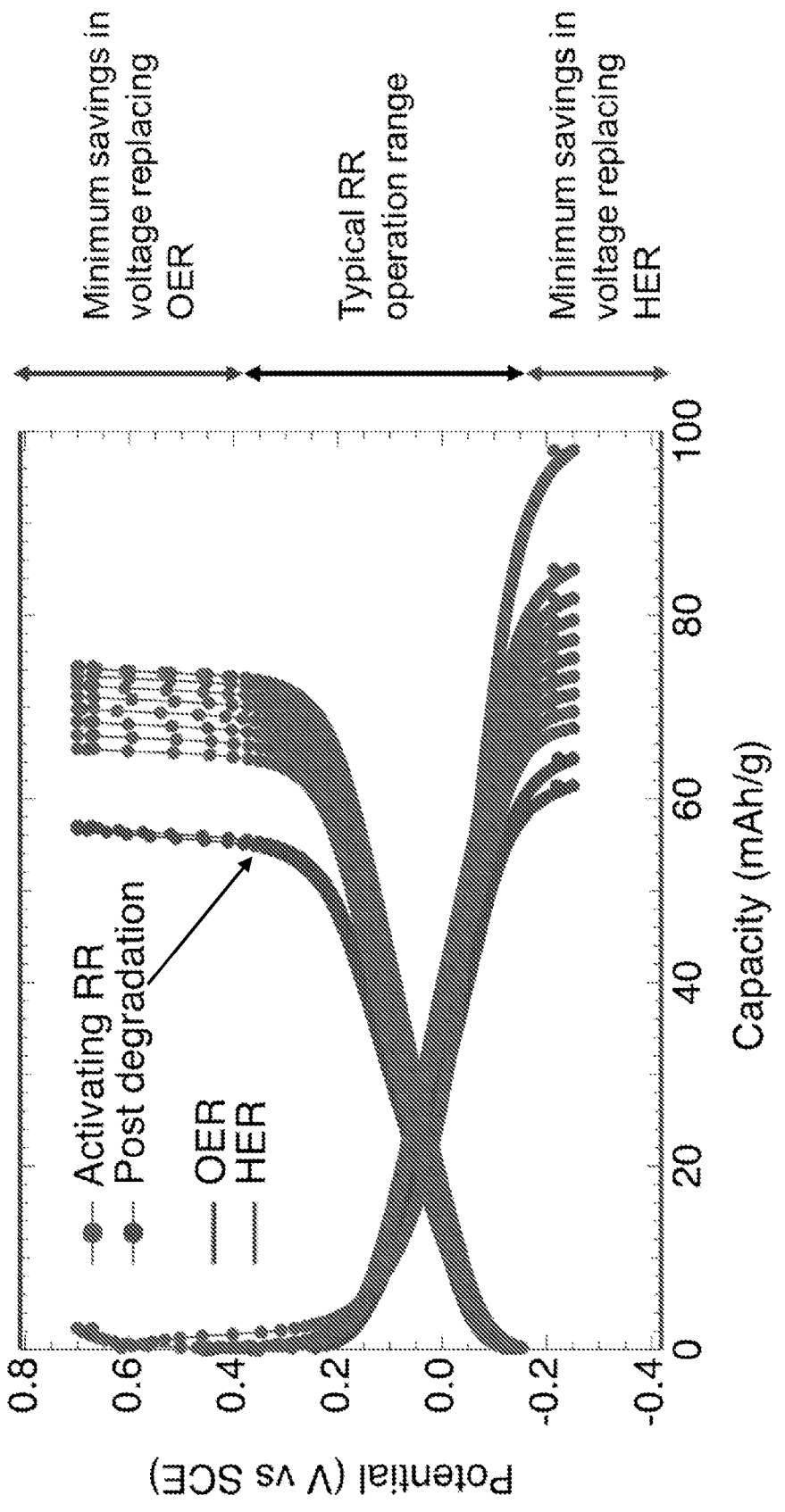
Minimum savings in voltage replacing OER
Typical RR operation range
Minimum savings in voltage replacing HER
Activating RR
Post degradation
OER
HER
Potential (V vs SCE)
0.8
0.6
0.4
0.2
0.0
-0.2
-0.4
0
20
40
60
80
100
Capacity (mAh/g)

FIG. 7

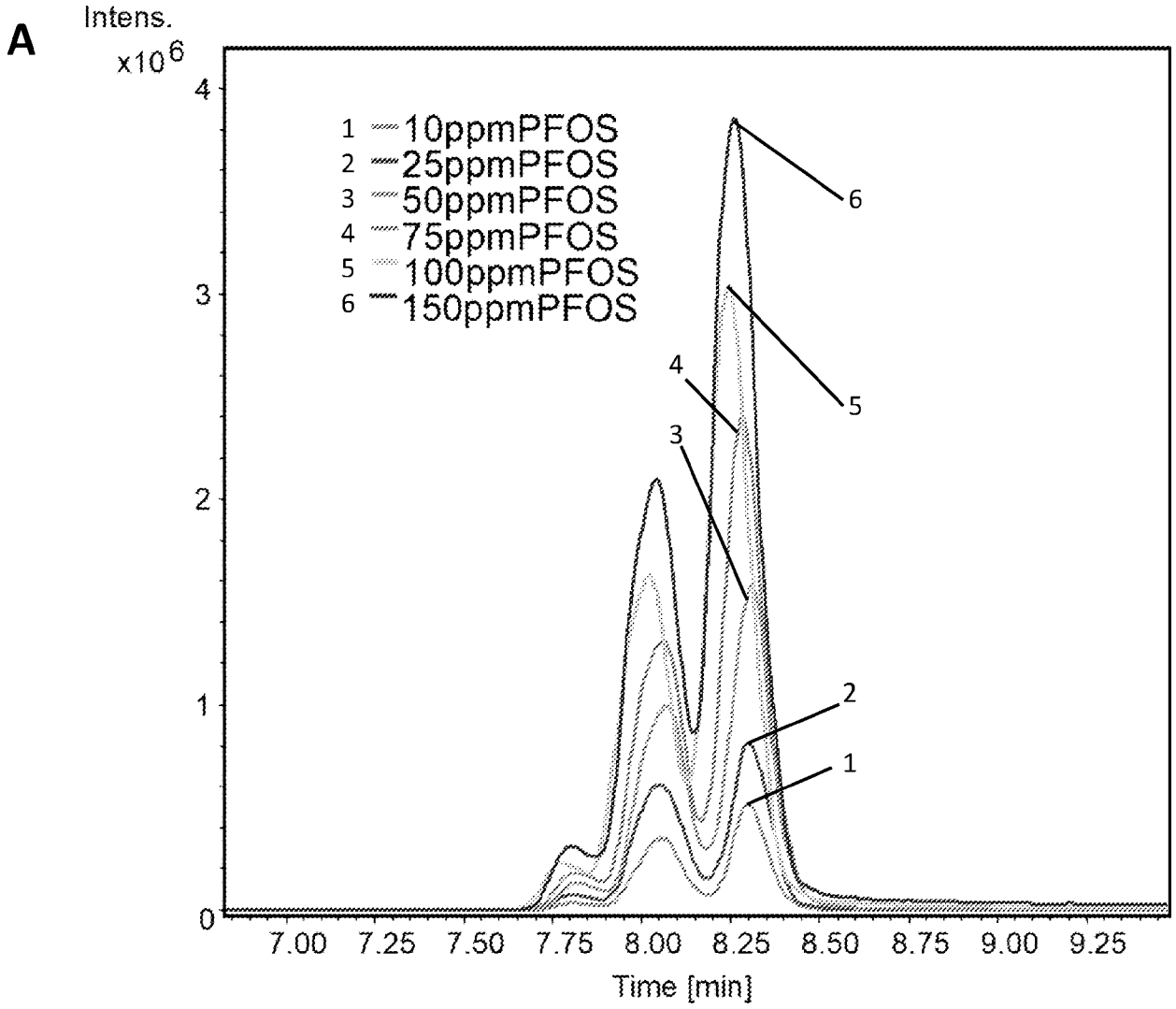
A
Intens.
x10^6
4
3
2
1
0
1 10ppmPFOS
2 25ppmPFOS
3 50ppmPFOS
4 75ppmPFOS
5 100ppmPFOS
6 150ppmPFOS
6
5
4
3
2
1
7.00
7.25
7.50
7.75
8.00
8.25
8.50
8.75
9.00
9.25
Time [min]

FIG. 8

B

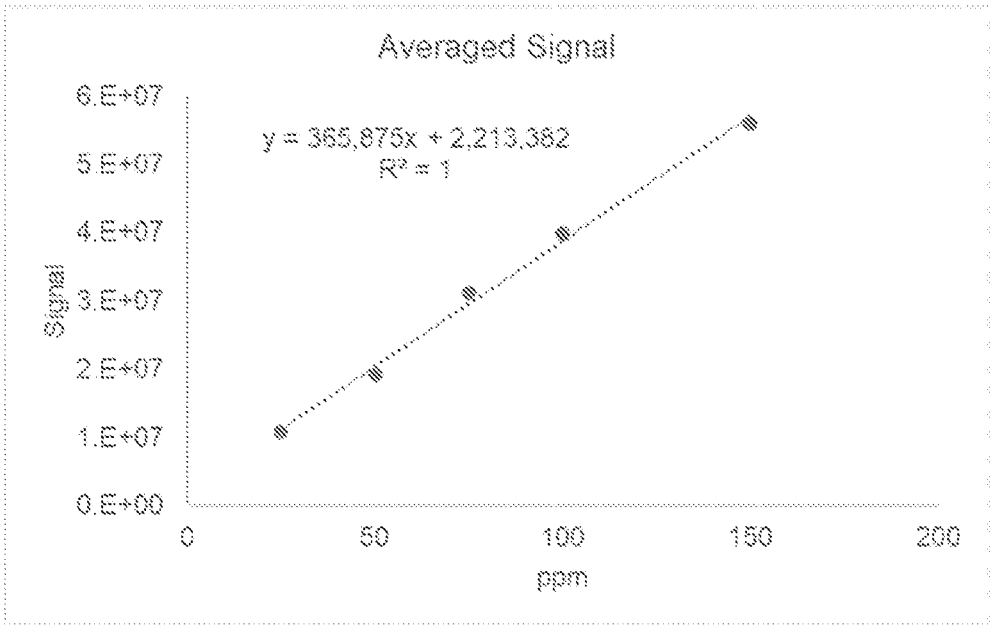

C

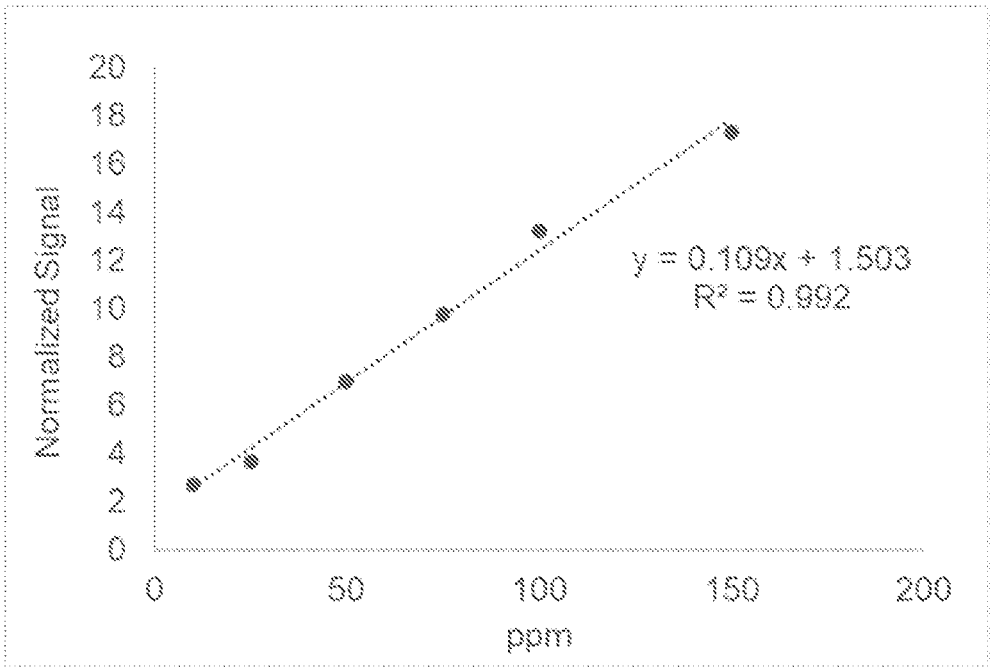

FIG. 8 cont'd

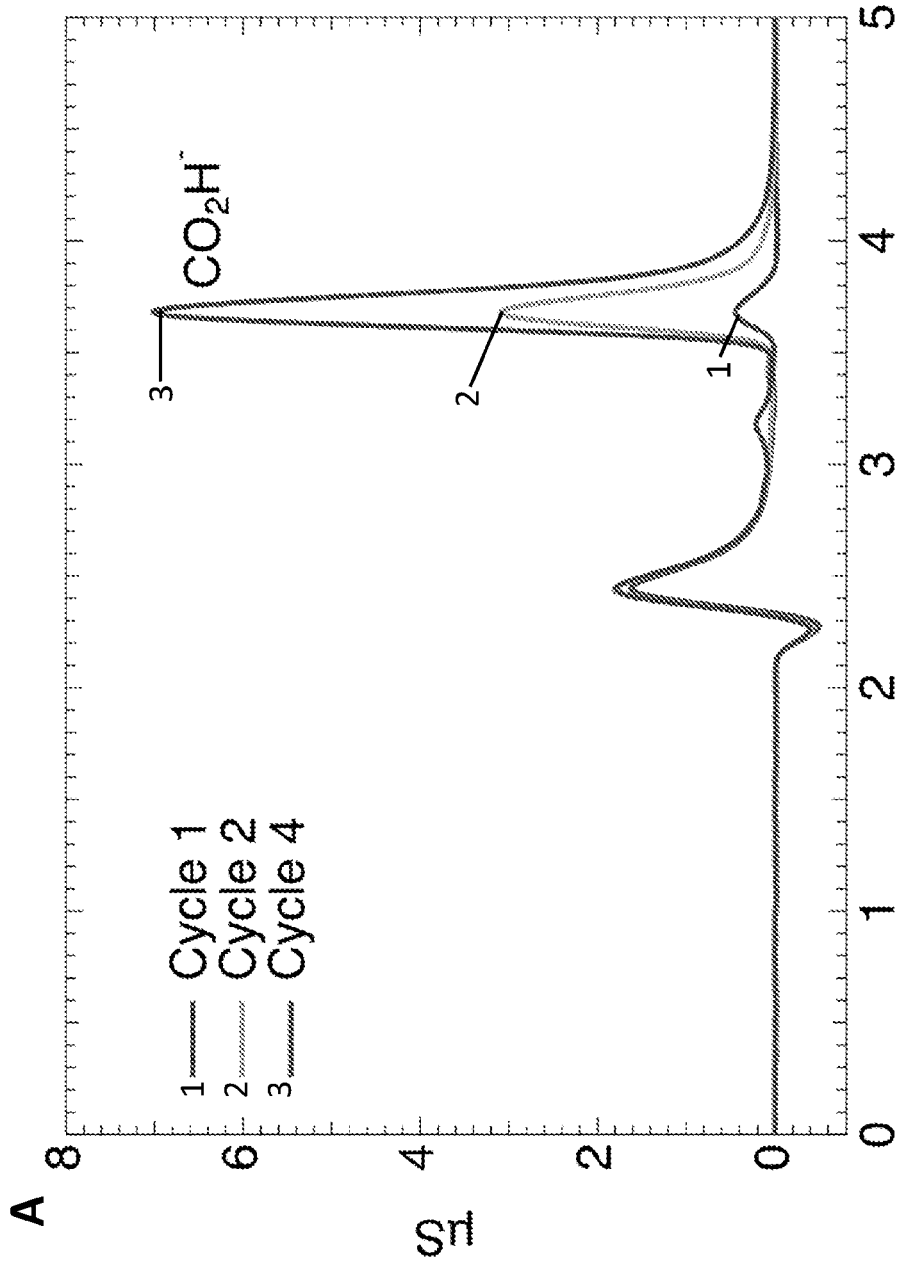
A
8
6
4
2
0
SrI
0
1
2
3
4
5
Time (min)
1 Cycle 1
2 Cycle 2
3 Cycle 4
CO_2H^-
1
2
3

FIG. 9

B

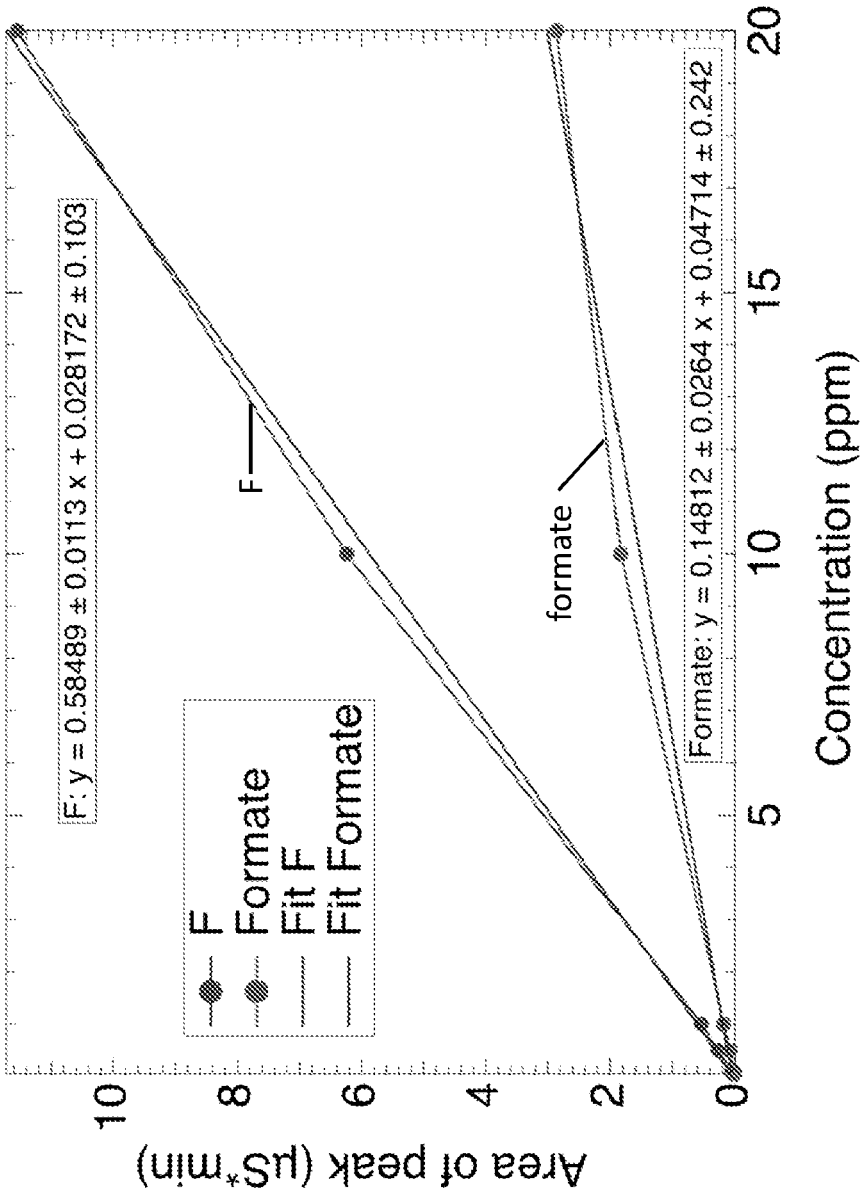
Area of peak (µS*min)
Concentration (ppm)
F
Formate
Fit F
Fit Formate
F: y = 0.58489 ± 0.0113 x + 0.028172 ± 0.103
Formate: y = 0.14812 ± 0.0264 x + 0.04714 ± 0.242
F
formate
0
2
4
6
8
10
5
10
15
20

FIG. 9 cont'd

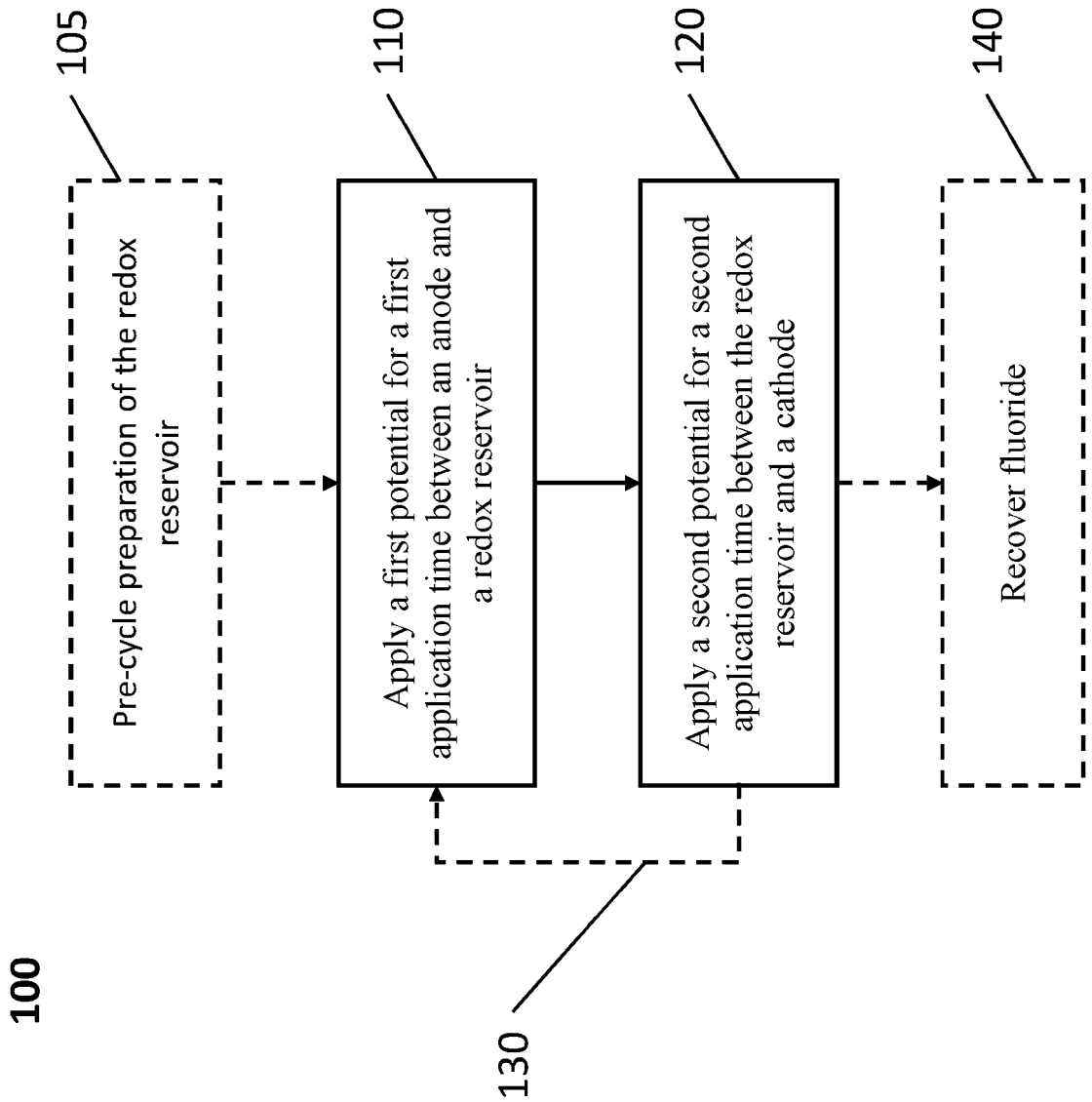
100
105
Pre-cycle preparation of the redox reservoir
110
Apply a first potential for a first application time between an anode and a redox reservoir
120
Apply a second potential for a second application time between the redox reservoir and a cathode
130
140
Recover fluoride

FIG. 10

INTERNATIONAL SEARCH REPORT

International application No.
PCT/US2025/027892

A. CLASSIFICATION OF SUBJECT MATTER

IPC: ***C02F 1/58*** (2025.01); ***C25B 1/29*** (2025.01); ***C25B 1/30*** (2025.01); ***C25B 3/23*** (2025.01); ***C25B 3/25*** (2025.01); ***A62D 3/115*** (2025.01); ***A62D 3/34*** (2025.01); ***C02F 1/467*** (2025.01)

CPC: ***C02F 1/583; A62D 3/115; A62D 3/34; C02F 1/46104; C02F 1/467; C25B 1/29; C25B 1/30; C25B 3/23; C25B 3/25;*** *C02F 2101/36*

According to International Patent Classification (IPC) or to both national classification and IPC

B. FIELDS SEARCHED

Minimum documentation searched (classification system followed by classification symbols)

See Search History Document

Documentation searched other than minimum documentation to the extent that such documents are included in the fields searched

See Search History Document

Electronic data base consulted during the international search (name of data base and, where practicable, search terms used)

See Search History Document

C. DOCUMENTS CONSIDERED TO BE RELEVANT

Category*	Citation of document, with indication, where appropriate, of the relevant passages	Relevant to claim No.
Y	CN 114715980 B (TONGJI UNIVERSITY) 08 August 2023 (08.08.2023) see machine translation	1-3, 23-26
Y	US 2023/0322589 A1 (UNIVERSITY OF GEORGIA RESEARCH FOUNDATION INC.) 12 October 2023 (12.10.2023) entire document	26
A	US 5,643,437 A (DONG et al.) 01 July 1997 (01.07.1997) entire document	1-3, 23-26
Y	WANG et al., Modular Electrochemical Synthesis Using a Redox Reservoir Paired with Independent HalfReactions, Joule, Vol. 5, 20 January 2021 [retrieved on 13 August 2025]. Retrieved from the Internet: <URL: https://www.cell.com/joule/pdfExtended/S2542-4351(20)30555-9 >. Pgs. 149–165	1-3, 23-26

☐ Further documents are listed in the continuation of Box C. ☐ See patent family annex.

* Special categories of cited documents:
"A" document defining the general state of the art which is not considered to be of particular relevance
"D" document cited by the applicant in the international application
"E" earlier application or patent but published on or after the international filing date
"L" document which may throw doubts on priority claim(s) or which is cited to establish the publication date of another citation or other special reason (as specified)
"O" document referring to an oral disclosure, use, exhibition or other means
"P" document published prior to the international filing date but later than the priority date claimed
"T" later document published after the international filing date or priority date and not in conflict with the application but cited to understand the principle or theory underlying the invention
"X" document of particular relevance; the claimed invention cannot be considered novel or cannot be considered to involve an inventive step when the document is taken alone
"Y" document of particular relevance; the claimed invention cannot be considered to involve an inventive step when the document is combined with one or more other such documents, such combination being obvious to a person skilled in the art
"&" document member of the same patent family

Date of the actual completion of the international search	Date of mailing of the international search report
16 August 2025 (16.08.2025)	**22 August 2025 (22.08.2025)**

Name and mailing address of the ISA/US	Authorized officer
COMMISSIONER FOR PATENTS **MAIL STOP PCT, ATTN: ISA/US** **P.O. Box 1450** **Alexandria, VA 22313-1450** **UNITED STATES OF AMERICA**	**TAINA MATOS**
Facsimile No. **571-273-8300**	Telephone No. **571-272-4300**

INTERNATIONAL SEARCH REPORT

International application No.
PCT/US2025/027892

Box No. II Observations where certain claims were found unsearchable (Continuation of item 2 of first sheet)

This international search report has not been established in respect of certain claims under Article 17(2)(a) for the following reasons:

1. ☐ Claims Nos.:
because they relate to subject matter not required to be searched by this Authority, namely:

2. ☐ Claims Nos.:
because they relate to parts of the international application that do not comply with the prescribed requirements to such an extent that no meaningful international search can be carried out, specifically:

3. ☑ Claims Nos.: **4-22, 27-31**
because they are dependent claims and are not drafted in accordance with the second and third sentences of Rule 6.4(a).